Cerebral Cortex September 2012;22:2039–2054
doi:10.1093/cercor/bhr284
Advance Access publication October 10, 2011

Germinal Zones in the Developing Cerebral Cortex of Ferret: Ontogeny, Cell Cycle Kinetics, and Diversity of Progenitors

Isabel Reillo and Víctor Borrell

Instituto de Neurociencias, Consejo Superior de Investigaciones Científicas—Universidad Miguel Hernández, 03550 Sant Joan d'Alacant, Spain

Address correspondence to Víctor Borrell, Instituto de Neurociencias, Consejo Superior de Investigaciones Científicas—Universidad Miguel Hernández, Avenida Ramón y Cajal s/n, 03550 Sant Joan d'Alacant, Spain. Email: vborrell@umh.es.

Expansion and folding of the cerebral cortex are landmark features of mammalian brain evolution. This is recapitulated during embryonic development, and specialized progenitor cell populations known as intermediate radial glia cells (IRGCs) are believed to play central roles. Because developmental mechanisms involved in cortical expansion and folding are likely conserved across phylogeny, it is crucial to identify features specific for gyrencephaly from those unique to primate brain development. Here, we studied multiple features of cortical development in ferret, a gyrencephalic carnivore, in comparison with primates. Analyzing the combinatorial expression of transcription factors, cytoskeletal proteins, and cell cycle parameters, we identified a combination of traits that distinguish in ferret similar germinal layers as in primates. Transcription factor analysis indicated that inner subventricular zone (ISVZ) and outer subventricular zone (OSVZ) may contain an identical mixture of progenitor cell subpopulations in ferret. However, we found that these layers emerge at different time points, differ in IRGC abundance, and progenitors have different cell cycle kinetics and self-renewal dynamics. Thus, ISVZ and OSVZ are likely distinguished by genetic differences regulating progenitor cell behavior and dynamics. Our findings demonstrate that some, but not all, features of primate cortical development are shared by the ferret, suggesting a conserved role in the evolutionary emergence of gyrencephaly.

Keywords: neurogenesis, OSVZ, Pax6, phosphovimentin, Tbr2

Introduction

Tangential expansion and folding of the cerebral cortex are landmark features of mammalian brain evolution, which are thought to underlie the growth of intellectual capacity. Accordingly, human mutations causing a loss of cortical convolutions (lissencephaly) or a decrease in brain size (microcephaly), result in severe reductions of intellectual performance (Ross and Walsh 2001; Sheen and Walsh 2003; Bilguvar et al. 2010; Nicholas et al. 2010; Yu et al. 2010). In primates, including human, expansion and folding of the cerebral cortex take place largely during fetal development (Bayer and Altman 2005). This process is believed to be critically dependent on the action of progenitor cells found in the outer subventricular zone (OSVZ), a specialized germinal layer characteristic of the fetal primate cerebral cortex (Rakic 1988, 1995, 2009; Smart et al. 2002; Kriegstein et al. 2006; Dehay and Kennedy 2007). Because cortical expansion and folding are not unique to primates but rather common across mammalian phylogeny (Welker 1990), we and others have proposed that the OSVZ may not be unique to primates but a feature distinctive of species with a folded cerebral cortex (gyrencephalic) (Fietz et al. 2010; Reillo et al. 2011). Indeed, several studies demonstrate the existence of a prominent OSVZ-like germinal layer in a variety of nonprimate gyrencephalic species, including ferret (Fietz et al. 2010; Reillo et al. 2011), cat, and sheep but not in lissencephalic species like mouse and guinea pig (Reillo et al. 2011; but see Shitamukai et al. 2011; Wang et al. 2011).

Cell lineage analyses demonstrate that the OSVZ plays fundamental roles in cortical development of gyrencephalic species, including neurogenesis and the tangential dispersion of radially migrating neurons (Hansen et al. 2010; Reillo et al. 2011). However, the defining features of the different germinal layers in the cerebral cortex of nonprimate gyrencephalic species, and how similar are these germinal layers from their primate counterparts, are poorly understood (Molnar et al. 2011; Reillo et al. 2011). Because the basic developmental mechanisms involved in cortical expansion and folding are likely conserved across mammalian phylogeny (Reillo et al. 2011), understanding the differences and similarities between developing primate and nonprimate gyrencephalic brains is fundamental to distinguish between the features relevant for the development of gyrencephaly and features evolved specifically for primate brain development (Dorus et al. 2004; Evans et al. 2004; Gilbert et al. 2005; Mekel-Bobrov et al. 2005; Pollard et al. 2006).

In lissencephalic rodents, like mouse and guinea pig, cortical progenitors are organized in 2 germinal layers: the ventricular zone (VZ) housing radial glia progenitors and the subventricular zone (SVZ) housing neurogenic intermediate progenitors (also termed secondary, abventricular, or basal progenitors) (Bayer and Altman 1991; Takahashi et al. 1995; Malatesta et al. 2000; Noctor et al. 2001, 2004; Martinez-Cerdeno et al. 2006; Kowalczyk et al. 2009; Reillo et al. 2011). In mouse, VZ progenitors are defined by expression of the transcription factor Pax6 and not Tbr2 (Pax6+/Tbr2–), while SVZ progenitors are Tbr2+/Pax6– (Englund et al. 2005; Hevner et al. 2006; Kowalczyk et al. 2009). In gyrencephalic primates, the SVZ is much thicker than in rodents and is subdivided into inner and outer SVZ (ISVZ and OSVZ), separated from each other by an inner fiber layer (IFL), and limited superficially by the intermediate zone (IZ) (also named outer fiber layer [OFL] or honeycomb matrix-like layer) (Smart et al. 2002; Bayer and Altman 2005; Zecevic et al. 2005; Bystron et al. 2006; Dehay and Kennedy 2007; Bayatti, Moss, et al. 2008; Bayatti, Sarma, et al. 2008; Reillo et al. 2011). The cellular and molecular composition of the different germinal zones in the human fetus cerebral cortex have been defined and characterized to some extent. In particular, the OSVZ is known to be a very complex

layer containing a highly heterogeneous population of cortical progenitors expressing different combinations of Pax6, Tbr2, Olig2, Sox2, and other genes and also containing radially and tangentially migrating neurons, radial glia and axonal fibers, displaced radial glia cells, and radial glia–like cells (oRGs/IRGCs) (Sidman and Rakic 1973; Letinic et al. 2002; deAzevedo et al. 2003; Zecevic 2004; Zecevic et al. 2005; Bystron et al. 2006; Howard et al. 2006; Mo et al. 2007; Bayatti, Moss, et al. 2008; Bayatti, Sarma, et al. 2008; Mo and Zecevic 2008, 2009; Hansen et al. 2010; Reillo et al. 2011).

To identify similarities and differences in cortical development between primate and nonprimate gyrencephalic species at the cellular and molecular levels, we have studied the composition of the germinal layers in the developing cerebral cortex of the ferret, a gyrencephalic carnivore. By analyzing the combinatorial expression of a wide variety of transcription factors, cell cycle factors, and cytoskeletal proteins, we have identified a combination of features that distinguish in ferret the same subdivisions of the germinative epithelium as in primates: VZ, ISVZ, and OSVZ. We also provide evidence for the existence of a vestigial form of the primate IFL in the ferret, which we identify as inner OSVZ (iOSVZ). We find that ferret ISVZ and OSVZ contain a nearly identical mixture of progenitor cell subpopulations as defined by transcription factor expression. However, in spite of having a common gene expression profile, ISVZ and OSVZ emerge at different developmental time points, differ in intermediate radial glia cell (IRGC) abundance, and their progenitors have different cell cycle kinetics and self-renewal dynamics, indicating the likely existence of yet unidentified genetic differences. Our findings demonstrate that some of the key traits characteristic of the primate germinal layers are shared by the ferret, while completely different than in mouse, suggesting that these features may be relevant to the developmental emergence of gyrencephaly.

Materials and Methods

Animals and Tissue Collection

Pigmented ferrets (*Mustela putorius furo*) were obtained from Marshall Bioresources (North Rose, NY) and kept on a 12:12 h light:dark cycle at the Animal Facilities of the Universidad Miguel Hernández, where animals were treated according with Spanish and European Union regulations, and experimental protocols were approved by the Universidad Miguel Hernández Institutional Animal Care and Use Committee. For embryonic stages, pregnant dams were deeply anesthetized with ketamine/xylazine induction followed by Isoflurane, and the embryos were extracted by cesarean section. All animals were perfused transcardially with phosphate-buffered 4% paraformaldehyde (PFA), and the brains postfixed in PFA.

Immunostaining

Single and double immunostains were performed on 50-μm thick free-floating cryosections or 5-μm thick paraffin sections in the parasagittal plane. After antigen retrieval, sections were blocked and incubated in primary antibodies overnight at 4 °C, then incubated with appropriate fluorescently conjugated secondary antibodies (Chemicon and Jackson), and counterstained with 4′,6-diamidino-2-phenylindole (SIGMA). Alternatively, sections were incubated with appropriate biotinylated secondary antibodies, with ABC complex (1:100, Vector), and developed with nickel enhancement as described elsewhere (Borrell et al. 1999). When necessary, sections were counterstained with Nissl solution. Primary antibodies and dilutions used are indicated in Supplementary Table 1. Quantification of cell costaining was performed by confocal microscopy (Leica) through a ×40 lens and ×4 zoom. Images were acquired from cells in A17 from 3 sections per subject, 2–3 subjects per age. Images were analyzed using ImageJ and Neurolucida software (Microbrightfield).

Cumulative Bromodeoxyuridine Labeling and Cell Cycle Analysis

One or multiple doses of bromodeoxyuridine (BrdU, SIGMA) were injected in ferret kits aged postnatal day (P) 0 or P6 ($n = 3$ animals per age) at 50 mg/kg body weight. For cell cycle length determination, BrdU was administered every 2 h for a total of 2 or 10 h, followed by transcardiac perfusion with PFA 1 h after the last injection. For each experimental group, the percentage of Ki67+ cells labeled with BrdU was calculated. The values of these measurements at 3 and 11 h defined a regression line that was used to calculate Tc-s (length of the cell cycle minus S-phase; time required to label 100% of progenitor cells with BrdU) and Ts (time at which 0% of Ki67+ cells would be labeled with BrdU) (Fig. 7). Tc was defined as Tc-s + Ts.

Results

Emergence and Distinction of Germinal Layers

To study the emergence and progression of the distinct germinal layers in the developing ferret cerebral cortex, we began by analyzing its general cytoarchitectural organization on Nissl stains between embryonic day (E) E30 and postnatal day (P) P14, focused on the prospective primary visual cortex. This window of developmental time includes the period when the germinal layers exhibit their largest size (Martinez-Cerdeno et al. 2006; Reillo et al. 2011) and the period of neurogenesis for all layers in this area of the ferret cerebral cortex (Jackson et al. 1989). During this period of development, and particularly at postnatal stages, we distinguished up to 8 different cytoarquitectonic subdivisions of the cerebral cortex, based on cell density and general organization (Fig. 1), which we named on the basis of current nomenclature for the developing primate cerebral cortex (Boulder Committee 1970; Bystron et al. 2008).

At E30, the prospective visual (occipital) cortex was formed namely by a VZ, characterized by containing a high density of cells with an elongated soma and columnar arrangement and limiting with the telencephalic lateral ventricle. The VZ was overlaid by a thin SVZ, characteristically formed by a high density of small rounded cells with no particular orientation or organization. A very thin cortical plate (CP), of only 2 or 3 cell diameters in thickness, was also distinguishable intercalated between 2 cell-sparse layers: marginal zone (MZ) and subplate (SP) zone/IZ overlaying the SVZ (Fig. 1*B*). Four days later, at E34, only the same 5 layers were still distinguishable, although the SVZ, SP/IZ, and CP were much thicker than previously (Fig. 1*B*). E38 was the earliest stage at which subdivisions of the SVZ could be distinguished, which we identified as ISVZ and OSVZ (Fig. 1*B*). The ISVZ was similar to the SVZ of earlier stages, characterized by containing a high density of small rounded cells, whereas the OSVZ displayed a lower density of cells (Fig. 1*B*). In macaque monkey, ISVZ and OSVZ are separated by a distinctive fiber layer (IFL) at late, but not early, stages of cortical development (Smart et al. 2002). Although no obvious fiber layer could be distinguished between ISVZ and OSVZ in the E38 ferret, the striking difference in cell packing between these zones forced us to make this distinction (Fig. 1*B*). Moreover, within the OSVZ, we distinguished 2 subdivisions: outer OSVZ (oOSVZ) and iOSVZ, where the oOSVZ had a slightly higher cell density than the iOSVZ, and cells in the iOSVZ were aligned in radial streams (Fig. 1*B*; Supplementary Fig. 1). Cell streams in iOSVZ were only 1 or 2 cells in thickness

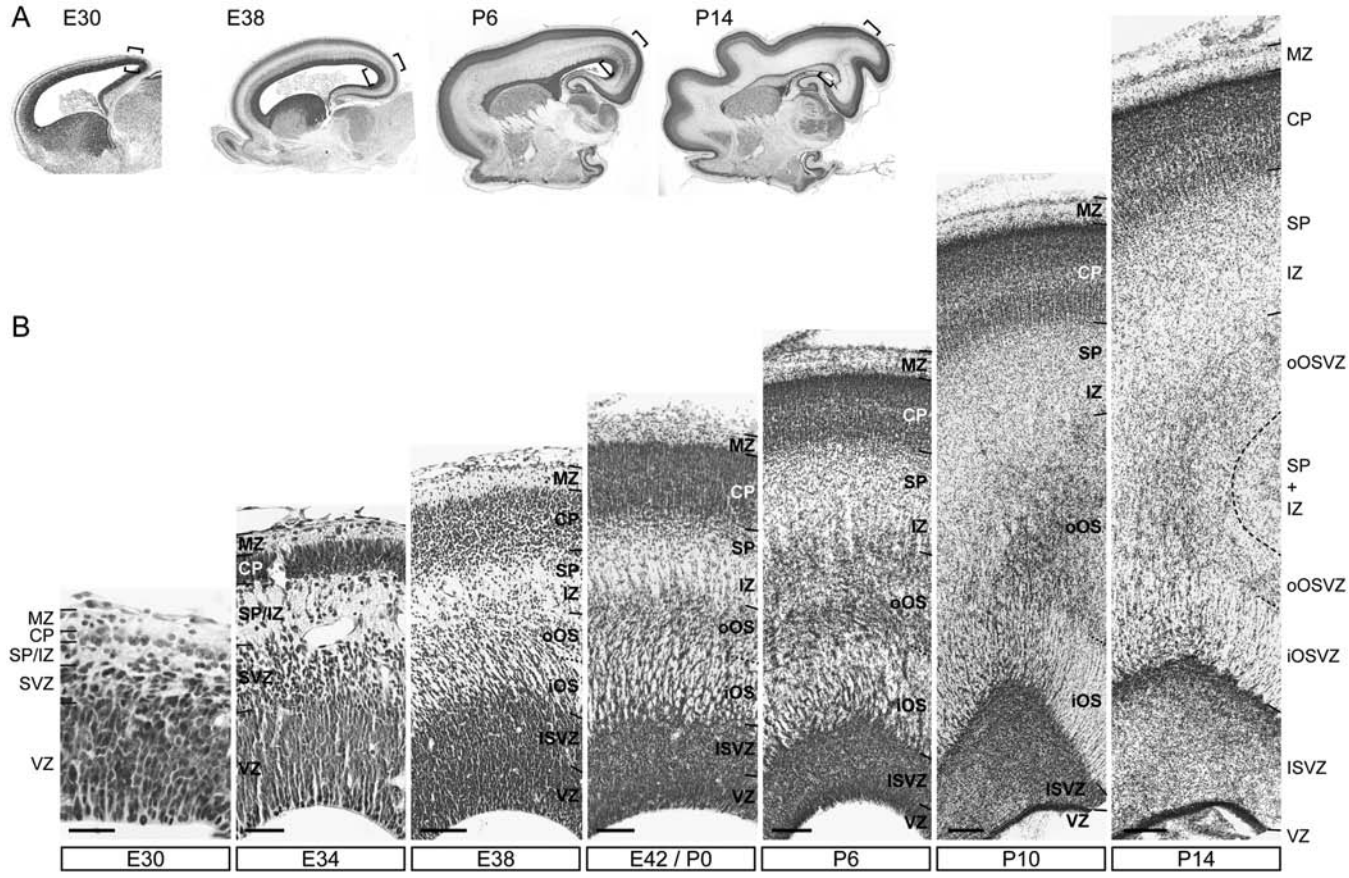

Figure 1. Ontogeny of the germinal layers in the ferret cerebral cortex. (*A*) Nissl stains of sagittal sections across the brain of developing ferrets at different stages of development. Brackets in (*A*) indicate regions shown in (*B*). (*B*) Details across the cortical depth of representative Nissl stains at different stages of development. At embryonic day (E) 30 and E34, a thin and disorganized SVZ is distinguishable from the columnar VZ. At E38, differences in cell density distinguish the SVZ into ISVZ and OSVZ, which is additionally subdivided in an iOS or iOSVZ and an oOS or oOSVZ. At postnatal stages (P), the thickness of the VZ decreases, while all other layers become thicker, including ISVZ, OSVZ, IZ, SP, and CP. Scale bars—50 μm (E30 and E34), 150 μm (E38 and E42), 200 μm (P6 and P10), and 300 μm (P14).

(Supplementary Fig. 1), and reminded of the progenitor cell streams observed in the human SVZ (Rakic and Zecevic 2003; Zecevic et al. 2005). Therefore, the OSVZ was subdivided from the onset in oOSVZ and iOSVZ (Fig. 1*B*).

The pattern of Nissl stain in the ISVZ at E38 was very similar to that of the SVZ at E34 (Fig. 1*B*), suggesting that the ISVZ may emerge first in development and the OSVZ later. This notion was further supported by examination of rostro-caudal differences in germinal layer organization, related to the corresponding gradient of cortical development (Fig. 2*A*). In contrast to the prospective visual cortex at caudal levels, at rostral levels, E34 embryos exhibited a cell-dense ISVZ and a cell-sparse OSVZ (Fig. 2*B,C*). Comparison from rostral to caudal levels showed that the ISVZ at rostral levels was continued with the SVZ at caudal levels as described above, whereas the OSVZ eventually disappeared (Fig. 2*A*–*C*). Taken together, these observations suggested that the emergence of the OSVZ at midstages of development may occur as a specialization from the ISVZ, as it may have occurred during mammalian evolution (Reillo et al. 2011).

Starting at E42/P0, and for the subsequent stages of postnatal development, 8 different cortical layers or subdivisions were clearly distinguishable by Nissl stain: VZ, ISVZ, iOSVZ, oOSVZ, IZ, SP, CP, and MZ (Fig. 1*B*). The deep layers VZ, ISVZ, iOSVZ, and oOSVZ had a similar appearance to previous stages. The IZ was characterized by a very low cell density, which at postnatal stages typically displayed a honeycomb matrix-like organization (Fig. 1*B*), reminiscent of the primate outer fiber layer (Smart et al. 2002; Bayer and Altman 2005; Zecevic et al. 2005). The SP had a graded distribution of cells with an overall density higher than the IZ. The CP contained a high density of large cells with a columnar arrangement; at postnatal stages, differentiating layers 6 and 5 could be also distinguished from the immature CP proper, but for simplicity, we maintained the nomenclature CP to include all postmigratory neuronal layers that will differentiate into layers 2–6 of the mature cerebral cortex. Finally, the MZ was characterized by containing a very low density of cells and limiting with the pial surface of the cerebral cortex (Fig. 1*B*).

Between E30 and P14, the thickness of the VZ decreased gradually, concomitant with a gradual increase in the thickness of most other layers (Fig. 1*B* and Table 1). Thickness increase was particularly accentuated in the ISVZ and oOSVZ, while it was much less pronounced in the other layers (Fig. 1, P10 and P14; Table 1). Moreover, starting at P6, the layers between oOSVZ and MZ suffered significant bending and deformation, related to the incipient folding of the cortical mantle during this period (Fig. 1*A,B*) (Smart and McSherry 1986; Neal et al. 2007; Reillo et al. 2011). Altogether, the above results revealed the existence in the developing ferret cerebral cortex of 7 distinct cortical layers, of which the OSVZ was subdivided into

inner and outer subzones, and suggested that the early forming SVZ may later become ISVZ and give rise to the OSVZ.

Patterns of Cell Proliferation Differ between Germinal Layers and Developmental Stages

To demonstrate which of the cytoarchitectonic subdivisions identified by Nissl stain corresponded to germinal layers, we next studied the patterns of cell proliferation. To this aim, we analyzed the expression pattern of 3 different markers: PH3, which labels the DNA of cells in mitosis; Ki67 antigen, labeling cells in cell cycle; and Sox2, a neural stem/progenitor cell marker (Hansen et al. 2010). We also used BrdU administration with short survival time to reveal progenitors in S-phase of the cell cycle. Cells positive for all 4 antigens were detected abundantly throughout the VZ, ISVZ, and OSVZ at all embryonic and/or postnatal stages analyzed, demonstrating that these 3 layers contain large amounts of cycling and mitotic progenitors and, thus, confirming that they are major germinal layers (Figs 3 and 4). Cells positive for PH3 (PH3+), Ki67, BrdU,

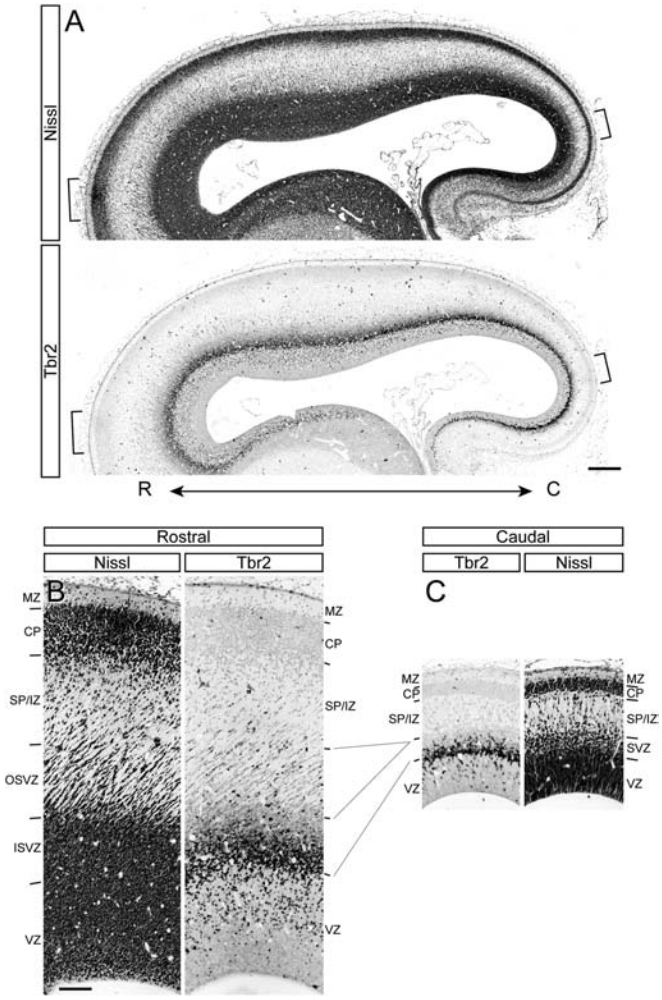

Figure 2. Gradient of SVZ development in the embryonic ferret. (*A*) Sagittal sections along the rostro-caudal extent of the E34 cortex stained for Nissl substance and Tbr2. Brackets indicate regions shown in (*B* and *C*). R, rostral; C, caudal. (*B* and C) Details of the rostral and caudal regions of the cerebral cortex shown in (*A*), illustrating differences in SVZ size and complexity. The cytoarchitecture and pattern of Tbr2+ cell distribution characteristic of the caudal SVZ extend rostrally to become ISVZ, whereas the rostral OSVZ does not have an equivalent layer at caudal levels. Scale bars—250 μm (*A*) and 250 μm (*B* and *C*).

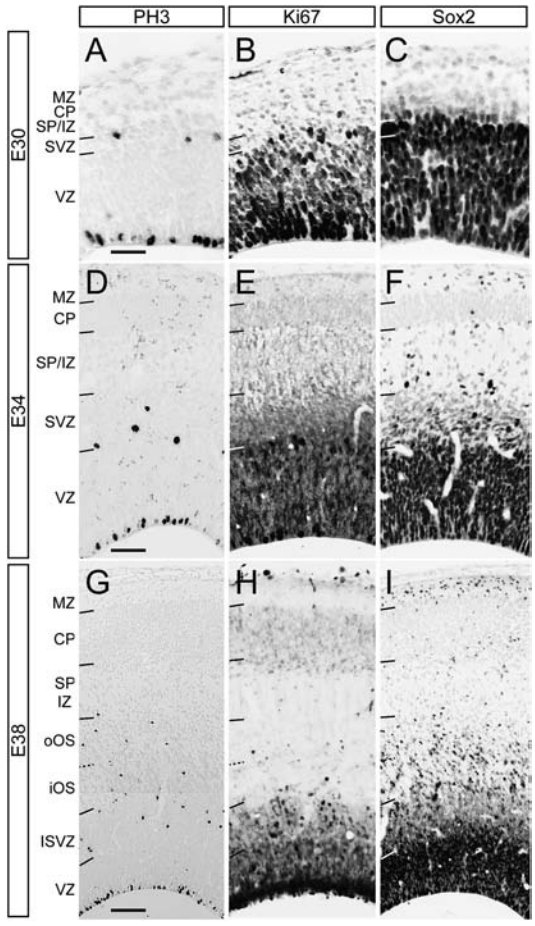

Figure 3. Ontogeny of germinal layers in the presumptive visual cortex of the embryonic ferret. Details across the cortical depth of representative stains for phosphohistone H3 (PH3) (*A*, *D*, and *G*), Ki67 (*B*, *E*, and *H*), and Sox2 (*C*, *F*, and *I*) at E30, E34, and E38. The SVZ and its multiple subdivisions are characterized by containing basal mitoses (PH3+ nuclei) and a low density of Ki67+ and Sox2+ cells. Scale bars—50 μm (E30 and E34) and 150 μm (E38).

Table 1
Thickness of cortical layers in the developing ferret cerebral cortex

	VZ	ISVZ	iOSVZ	oOSVZ	IZ-SP	CP
P0	96.6 ± 5.7	176.2 ± 8.5	173.6 ± 17.7	184.5 ± 19.7	228.2 ± 02	255.9 ± 331
P2	89.0 ± 30	179.3 ± 24.3	228.7 ± 14.8	207.2 ± 11.4	228.8 ± 5.4	314.7 ± 42.9
P6	73.6 ± 6.4	296.5 ± 340	368.3 ± 325	453.0 ± 37.8	337.2 ± 135	426.3 ± 37.9
P10	56.3 ± 117	608.2 ± 55.3	551.2 ± 577	1218.6 ± 689	565.8 ± 355	726.5 ± 106.9
P14	33.3 ± 4.6	580.3 ± 25.3	536.4 ± 37.6	2647.2 ± 213.5	854.6 ± 102.8	1073.3 ± 60.8

Note: At each postnatal stage (P), values indicate mean ± standard error of the mean in microns (n = 2–3 animals/stage).

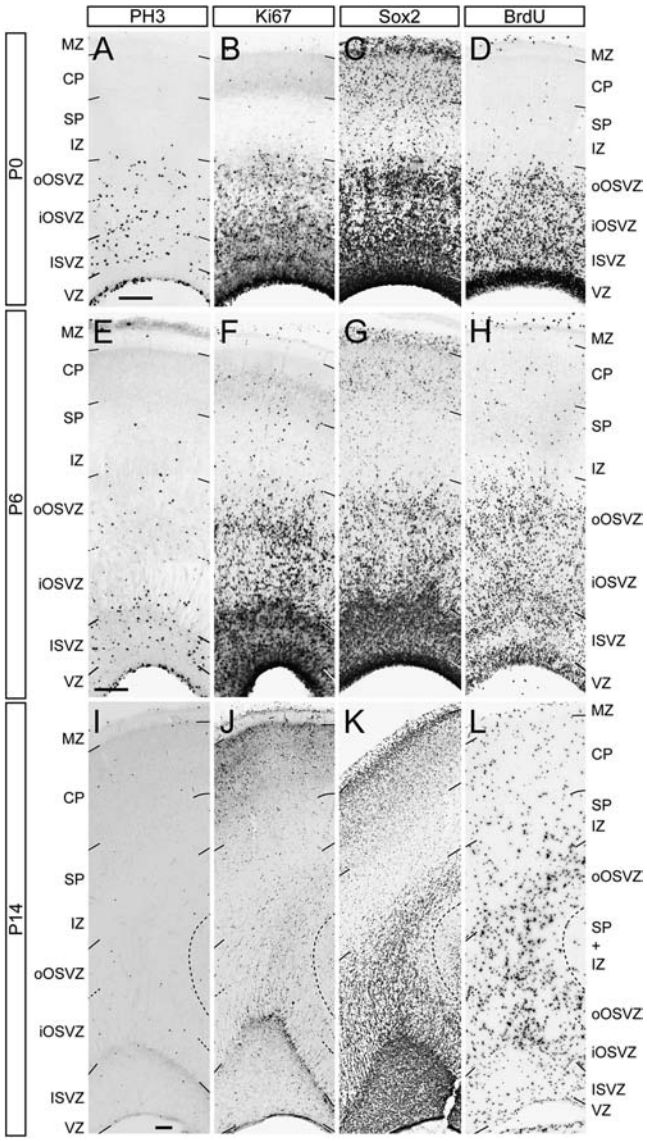

Figure 4. Ontogeny of germinal layers in the presumptive visual cortex of the postnatal ferret. Details across the cortical depth of representative stains for phosphohistone H3 (PH3) (*A*, *E*, and *I*), Ki67 (*B*, *F*, and *J*), Sox2 (*C*, *G*, and *K*), and BrdU (*D*, *H*, and *L*) at P0, P6, and P14. ISVZ and OSVZ are characterized by containing basal PH3+ nuclei. At P0 and P6, the OSVZ is distinguished from the ISVZ by having a lower density of Ki67+, Sox2+, and BrdU+ cells. Within the OSVZ, positive cells are at a higher density in the oOSVZ than in the iOSVZ. At P14, PH3+, Ki67+, and BrdU+ cells accumulate preferentially at the border between ISVZ and OSVZ and along the center of OSVZ. At all ages, Sox2+ cells are abundant in MZ. Scale bar—200 μm.

and particularly Sox2 were also observed in the IZ, CP, and MZ but in small numbers (Figs 3 and 4), indicating that these layers also contain some progenitors but are not major sites of proliferation.

The VZ was characterized throughout development by housing the highest density of PH3+, Ki67+, and Sox2+ cells, which were at a lower density in the ISVZ and the lowest in the OSVZ (Figs 3 and 4). In the ISVZ, BrdU+ cells accumulated preferentially in the outer half, next to the iOSVZ (Fig. 4*D*,*H*), unlike Ki67+ and Sox2+ cells that were homogeneously distributed (Fig. 4*B*,*C*,*F*,*G*). Within the OSVZ, the outer subzone (oOSVZ) contained a higher density of Ki67+, Sox2+, and BrdU+ cells than the iOSVZ, although this could reflect differences in cell density (Figs 1*B* and 4*B–D*,*F–H*). By P14, the density of PH3+, Ki67+, Sox2+, and BrdU+ cells had decreased dramatically (Fig. 4*I–L*), coincident with the end of the neurogenetic period in this cortical region (Jackson et al. 1989). Interestingly, whereas in the VZ, this decrease in cycling progenitors was paralleled by a decrease in thickness (Fig. 1*B* and Table 1), and in the ISVZ and OSVZ, this was paralleled by a dramatic increase in thickness (Fig. 1*B* and Table 1) and by the selective accumulation along the ISVZ–OSVZ border of the remaining progenitors (Fig. 4*I*,*J*). Taken together, these analyses confirmed the existence of VZ, ISVZ, and OSVZ as major germinal zones in the developing ferret cerebral cortex and that both subdivisions of the OSVZ (iOSVZ and oOSVZ) are highly proliferative. In addition, our BrdU labeling data suggested the possibility that progenitors in the ISVZ may be allocated to the outer or inner domains of this layer depending on their phase of the cell cycle, as occurs in the VZ due to the interkinetic nuclear migration of progenitor radial glia cells (Sauer and Walker 1959; Angevine and Sidman 1961; Takahashi et al. 1993).

Gene Expression Profiling of Developing Cortical Layers

The above findings demonstrated that cortical progenitors in the developing ferret are organized in 4 laminar subdivisions: VZ, ISVZ, iOSVZ, and oOSVZ. This prompted us to investigate what is the cellular and molecular basis of such a diverse and elaborate anatomical organization. Previous studies have distinguished distinct classes of cortical progenitors based on the expression profile of specific transcription factors, which usually correlate with distinct progenitor fate potentials (Haubensak et al. 2004; Noctor et al. 2004; Kowalczyk et al. 2009; Hansen et al. 2010). In the ferret cerebral cortex, a variety of progenitor cells have been identified based on the combinatorial expression of Pax6 and/or Tbr2, suggesting again the coexistence of diverse progenitor cell types with different fate potentials (Fietz et al. 2010; Reillo et al. 2011). Thus, we decided to characterize the lineage potential of the different germinal layers in the developing ferret cerebral cortex, by studying the expression pattern of proteins characteristic of neuronal versus glial lineages. We began by studying the transcription factors Pax6, Tbr2 and Tbr1, and the antigen NeuN, which in the mouse cerebral cortex are expressed sequentially in the neuronal lineage and distinguish between radial glia (VZ) and intermediate (SVZ) progenitors (Englund et al. 2005; Hevner et al. 2006). At E30 and E34, virtually, all cells of the VZ expressed high levels of Pax6, as opposed to the SVZ where the majority expressed low levels of Pax6, with only a few scattered cells Pax6 high at E34 (Fig. 5*A*,*E*,*I*). In contraposition, Tbr2 expression was very scarce in the VZ and massive in the SVZ, already at E30 (Fig. 5*B*,*F*,*J*), reminiscent of the mouse embryonic neocortex (Englund et al. 2005; Hevner et al. 2006). Thus, at early embryonic stages, Pax6 and Tbr2 distinguished SVZ from VZ, which suggested that this early SVZ may contain mouse-like intermediate progenitor cells (IPCs). At E38, the ISVZ resembled the SVZ at E34, containing a high amount of Tbr2+ cells in an inner-to-outer gradient of staining intensity, plus a few Pax6+ cells (Figs 2*B*,*C* and 5*E*,*F*,*I*,*J*). In contrast, the OSVZ contained a salt-and-pepper distribution of Pax6+ and Tbr2+ cells, found at similar abundance (Fig. 5*I*,*J*). The similarities found between the ISVZ at E38 and the SVZ at E34 reinforced the notion that the ISVZ emerges during development before the OSVZ (Figs 1 and 2).

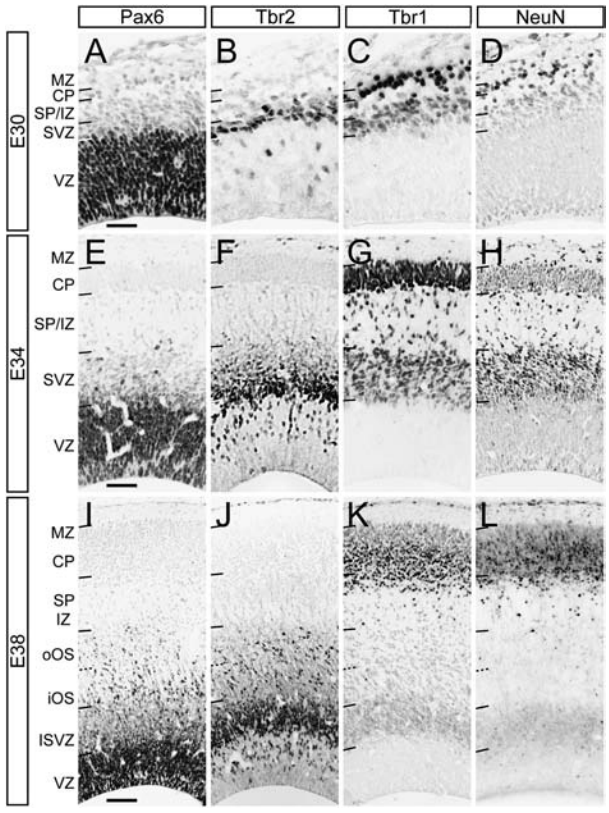

Figure 5. Ontogeny of transcription factor expression in the presumptive visual cortex of the embryonic ferret. Details across the cortical depth of representative stains for Pax6 (*A* ,*E*, and *I*), Tbr2 (*B*, *F*, and *J*), Tbr1 (*C*, *G*, and *K*), and NeuN (*D*, *H*, and *L*) at E30, E34, and E38. The embryonic SVZ and its subdivisions are characterized by containing a high abundance of Tbr2+ and Tbr1+ cells, occasinal Pax6+ cells, and cells weakly labeled for NeuN. Scale bars—50 μm (E30 and E34) and 150 μm (E38).

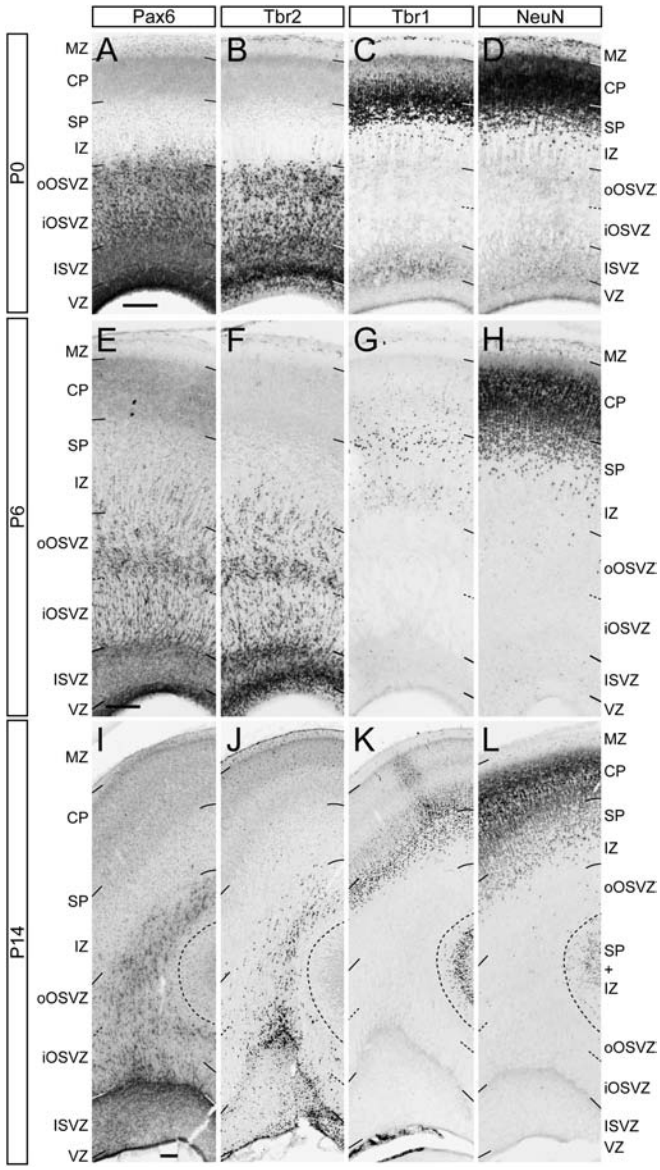

Figure 6. Ontogeny of transcription factor expression in the presumptive visual cortex of the postnatal ferret. Details across the cortical depth of representative stains for Pax6 (*A*, *E*, and *I*), Tbr2 (*B*, *F*, and *J*), Tbr1 (*C*, *G*, and *K*), and NeuN (*D*, *H*, and *L*) at P0, P6, and P14. ISVZ and OSVZ are characterized by containing a high abundance of Pax6+ and Tbr2+ cells. At P14, Pax6+, and Tbr2+ cells accumulate selectively at the border between ISVZ and OSVZ and along the center of the OSVZ. At P0, the ISVZ, but not OSVZ, also contains cells weakly labeled for Tbr1 and NeuN. At P6 and P14, Tbr1+ and NeuN+ cells are only in SP and CP. Scale bar—200 μm.

Between P0 and P6, Pax6 and Tbr2 presented similar expression patterns, with a high density of positive cells in VZ, ISVZ and OSVZ, and few scattered cells in the lower aspect of the IZ (Fig. 6*A,B,E,F*). In the VZ, Pax6 was homogeneously expressed, whereas the density of Tbr2+ cells increased gradually from the ventricular surface to the border with the ISVZ (Fig. 6*A,B,E,F*), similar to previous stages (Fig. 5*F,J*). In the ISVZ, Pax6 expression was again homogeneous, but Tbr2 staining distinguished 3 subdivisions, with cells in the middle third of this layer expressing lower levels of Tbr2 compared with those in the upper and lower thirds (Fig. 6*A,B,E,F*). This was in sharp contrast with the OSVZ, where Pax6+ and Tbr2+ cells had a very similar distribution distinguishing clearly the iOSVZ, with positive cells forming radial streams (Fig. 6*A,B,E,F* and Supplementary Fig. 1) from the oOSVZ with cells accumulating at high density and without an obvious organization (Fig. 6*A,B,E,F*). The alignment of Pax6+ and Tbr2+ cells in radial streams in the iOSVZ resembled the bands of cells described in the IFL of the embryonic cortex of macaque and human (Smart et al. 2002; Zecevic et al. 2005; Lukaszewicz et al. 2006), suggesting that these progenitors might be intermixed with bundles of axons (Supplementary Fig. 1). At P14, Pax6+ and Tbr2+ cells were much fewer than previously and accumulated preferentially in the interphase between ISVZ and OSVZ and also within the OSVZ following the curvature of the emerging splenial gyrus (Fig. 6*I,J*). The absence of Pax6+ or Tbr2+ cells in IZ, CP, and MZ at all stages suggested that the scattered cycling progenitors we had initially identified in these layers (Sox2+, BrdU+; see above) do not follow a neuronal lineage.

In contrast to Pax6 and Tbr2, Tbr1 and NeuN were expressed in both germinal and postmitotic layers and in highly dynamic patterns. Between E30 and E34, both Tbr1 and NeuN were expressed in CP, SP/IZ, and SVZ, being completely absent from the VZ (Fig. 5*C,D,G,H*). At E34, Tbr1 staining was strongest in CP and SP/IZ and then at lower levels in the SVZ (Fig. 5*G*). In contrast, the strongest NeuN labeling was found in SVZ and in scattered cells of IZ/SP and CP, while the majority of CP cells were weakly stained (Fig. 5*H*). Between E38 and P0,

the strongest Tbr1 and NeuN expression was confined to the lower part of CP and the SP, while cells in ISVZ, OSVZ, and IZ had very low expression levels, and cells in VZ were negative (Figs 5*K,L* and 6*C,D*). Finally, between P6 and P14, Tbr1+ cells were found exclusively in the SP (Fig. 6*G,K*), and NeuN+ cells occupied the entire thickness of the CP and SP (Fig. 6*H,L*). These observations suggested that young neurons migrating radially to the CP already expressed low levels of Tbr1 and NeuN, in agreement with previous descriptions of mouse and human cerebral cortex (Englund et al. 2005; Bayatti, Moss, et al. 2008; Bayatti, Sarma, et al. 2008; Lui et al. 2011).

Radial glia cells, astrocytes, and oligodendrocyte precursors are essential constituents of the developing cerebral cortex (Ramón y Cajal 1911; Schmechel and Rakic 1979; Takahashi et al. 1990; deAzevedo et al. 2003; Zecevic 2004; Mo and Zecevic 2009). To identify progenitors and cells of the oligodendroglial and astroglial lineages in the developing cerebral cortex, we studied the patterns of expression of Olig2, Vimentin, and Glial Fibrillary Acidic Protein (GFAP) (Tekki-Kessaris et al. 2001; Mo and Zecevic 2009). Olig2 expression started at E38 with very few positive cells mainly in SP/IZ and OSVZ (Supplementary Fig. 2). The number of Olig2+ cells increased during the first postnatal week and then decreased to very few cells by P14 (Figs 7*B,F,J*). Olig2+ cell distribution was always scattered and fairly homogeneous and involved not only the 3 main germinal zones but also the IZ, SP, CP, and MZ (Fig. 7*B,F,J*). This was in agreement with our earlier observations of few scattered cells in SP, CP, and MZ positive for Ki67, Sox2, and BrdU but negative for Pax6 and Tbr2 (Figs 3–6), strongly suggesting that progenitors in those layers belong mostly to the glial lineage.

Anti-vimentin immunostaining evidenced the organization of the radial fiber scaffold in the postnatal ferret cerebral cortex (Fig. 7*C,G,K*), as in other carnivores (Engel and Muller 1989; Voigt 1989). Staining of radial fibers by vimentin was very strong at P0 and P6, but much weaker at P14, when this protein was abundantly present in endothelial cells (Fig. 7*K*). We observed 2 types of organization of vimentin+ processes: Radial fibers following straight and largely parallel courses or processes with a highly wavy and disorganized appearance. Wavy fibers characterized the ISVZ and oOSVZ, whereas parallel fibers were typical in the other layers, including VZ, iOSVZ, IZ, and CP (Fig. 7*C,G,K* and Supplementary Fig. 3). Of note, vimentin+ fibers typically clustered in thick bundles in iOSVZ and IZ, remaining individualized in the other layers (Supplementary Fig. 3). Co-stains with anti-vimentin and anti-PH3 antibodies demonstrated that 87–94% of mitotic cells in VZ, ISVZ, and OSVZ were vimentin+ (P0, 148 of 157 cells; P6, 118 of 135 cells; Fig. 10*A–C*). Because at these stages cortical neurogenesis is at its peak (Jackson et al. 1989; Reillo et al. 2011), these observations strongly suggested that vimentin expression is not exclusive to glial progenitors but extensive to the full diversity of cortical progenitors, such as radial glia.

GFAP expression increased between P0 and P14 reciprocally to the progressive decrease of vimentin staining, with GFAP+ cells and processes increasing in number during this period. GFAP+ astrocytes were first observed, although anecdotically, in the CP at P0 (Fig. 7*D*). By P6, they were numerous in the CP, SP, and IZ, and by P14, they were very abundant and widespread throughout most cortical layers (Fig. 7*H,L*). Remarkably, GFAP was also expressed in radial processes at the VZ and ISVZ starting at P6 (Fig. 7*H,L*), reminiscent of the expression in cortical radial glia in primates (Levitt and Rakic 1980).

Taken together, the patterns of expression of different transcription factors suggested that a variety of progenitor cell types coexist in the germinal layers of the postnatal ferret cerebral cortex but also suggested that ISVZ and OSVZ may contain very similar classes of progenitors. In contrast, the different structural arrangements of glial cells and processes we observed allowed for a clear anatomical distinction between ISVZ and OSVZ and also demonstrated basic differences in organization between the outer and inner subdivisions of the OSVZ. This prompted us to an in-depth investigation of the diversity of progenitor cell classes and of how abundantly are they represented in each germinal layer.

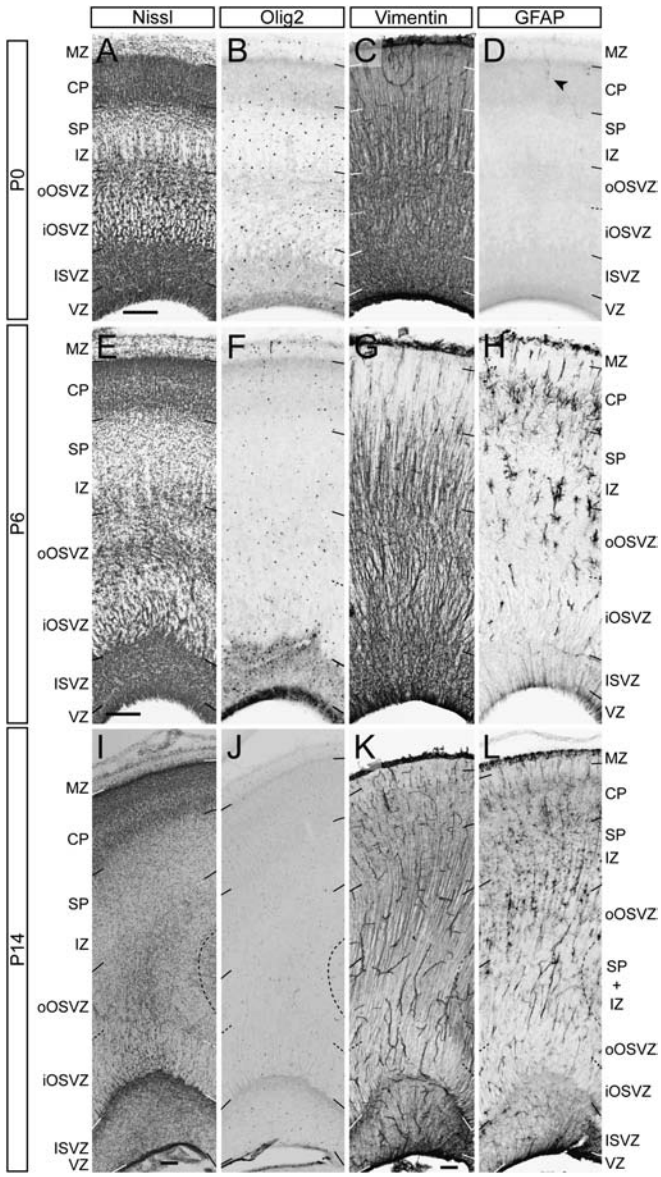

Figure 7. Ontogeny of glial marker expression in the presumptive visual cortex of the postnatal ferret. Details across the cortical depth of representative stains for Nissl (*A*, *E*, and *I*), Olig2 (*B*, *F*, and *J*), Vimentin (*C*, *G*, and *K*), and GFAP (*D*, *H*, and *L*) at P0, P6, and P14. Details in main text. Note the abundance of GFAP+ radial processes in VZ/ISVZ at P6 and P14. Scale bar—200 μm.

Progenitor Cells in ISVZ and OSVZ Share a Common Profile of Transcription Factor Expression

Previous analyses suggested that ISVZ and OSVZ have a similar composition of progenitor cell populations as defined by transcription factor expression (Reillo et al. 2011). However, ISVZ and OSVZ exhibit dramatic cytoarchitectonic differences throughout development, suggesting the existence of fundamental differences between cells of each layer. This apparent contradiction prompted us to refine our search for features that might distinguish between progenitor cells in ISVZ and OSVZ. In mouse, differential expression of the transcription factors Pax6 or Tbr2 distinguishes radial glia progenitors (VZ) from IPCs (SVZ) (Englund et al. 2005; Hevner et al. 2006; but see Shitamukai et al. 2011; Wang et al. 2011). In contrast, cortical progenitors in primates frequently coexpress Pax6, Tbr2, and/or other transcription factors, so multiple progenitor cell subclasses are distinguished by the combinatorial expression of these genes and coexist in the various germinal layers (Bayatti, Moss, et al. 2008; Mo and Zecevic 2008; Fietz et al. 2010; Hansen et al. 2010). We have previously shown that in the ferret cerebral cortex, the combinatorial expression of Pax6 and Tbr2 defines 4 subclasses of progenitor cells that coexist in similar proportions in the ISVZ and OSVZ (Reillo et al. 2011). This molecular similarity contrasts with our present findings that ISVZ and OSVZ have some very distinctive organizational features. Thus, we next attempted to explain those notorious differences between germinal layers in the cerebral cortex by extending the combinatorial analysis of transcription factor expression in progenitor cells to include Pax6, Tbr2, and Olig2 (Fig. 8*A–C*). We identified up to 7 different subclasses of progenitors at P0 and P6, expressing different combinations of the 3 transcription factors, although 2 of them were observed only anecdotically (Pax6+/Tbr2–/Olig2+ progenitors were never more than 1%; and Pax6–/Tbr2+/Olig2+ progenitors were only found at P6 and represented less than 0.5%; Fig. 8*D,E*). At P0, we found that in the VZ, 48% of progenitors were Pax6+ only, 6% were Tbr2+ only, 28% were Pax6+/Tbr2+/Olig2–, 2% expressed all 3 transcription factors, and 15% were negative for all 3 (Fig. 8*D*). In the ISVZ, we found the same subclasses of progenitors as in the VZ but represented in quite different proportions (Fig. 8*D*). In the OSVZ, we found the exact same progenitor subclasses as in the ISVZ and in strikingly similar proportions (Fig. 8*D*). Between P0 and P6, the relative abundance of the different progenitor cell populations changed significantly in the VZ: Progenitors expressing Pax6 alone increased up to 78%, while those that

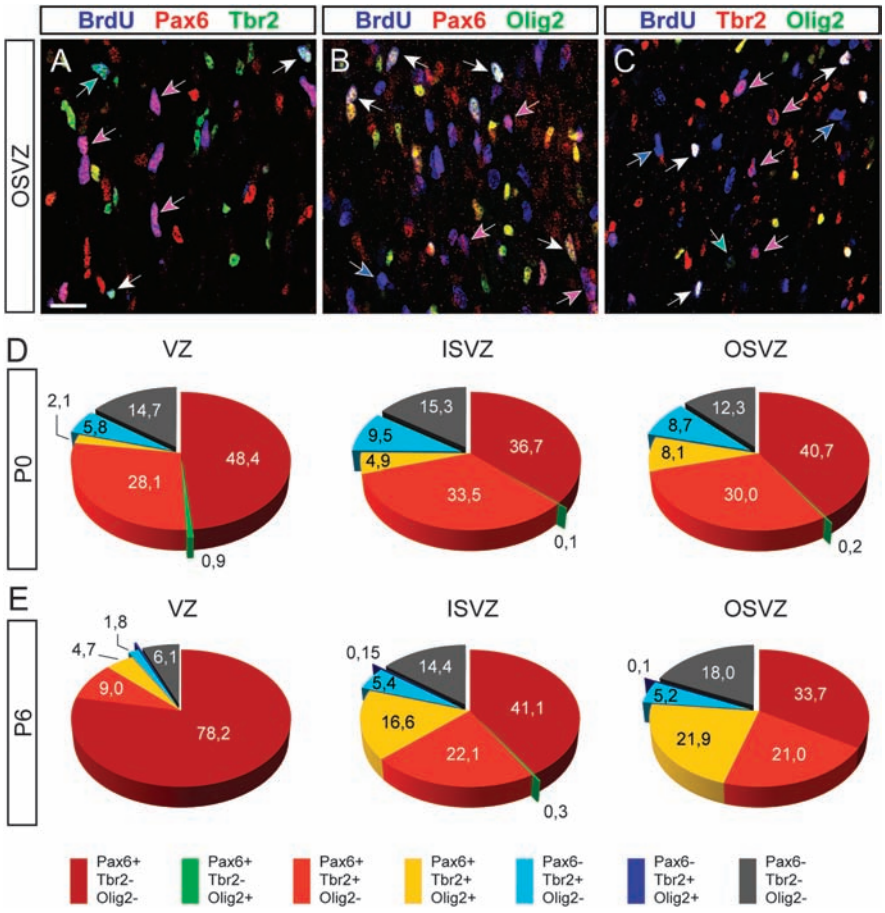

Figure 8. Transcription factor coexpression analysis in cortical progenitors of the prospective primary visual cortex at P6. (*A–C*) Different combinations of triple stains for BrdU, Pax6, Tbr2, and Olig2 in the OSVZ. Cycling progenitors are identified by BrdU stain (blue), and progenitor cells positive for different marker combinations are indicated by arrows color coded as in legend. (*D* and *E*) Quantification of the percentage of progenitors in the different proliferative layers at P0 (*D*) and P6 (*E*) expressing each of the marker combinations indicated in the color-coded legend. Progenitors in iOSVZ and oOSVZ were pooled. $n = 3$ animals per group, 3 sections per animal (P0, $n = 2957$ cells in VZ; 2092 cells in ISVZ; and 2870 cells in OSVZ. P6, $n = 2131$ cells in VZ; 2011 cells in ISVZ; and 3370 cells in OSVZ). Scale bar—20 μm.

were Pax6+/Tbr2+/Olig2– decreased down to 9%, and those negative for all 3 were only 6% (Fig. 8*E*). This shift observed in the VZ between P0 and P6 did not occur as dramatically in ISVZ or OSVZ, where only Pax6+/Tbr2+/Olig2+ progenitors increased (by 3-fold) in detriment of Pax6+/Tbr2+/Olig2– progenitors and of those expressing Tbr2 alone (Fig. 8*E*). Most importantly, the types and relative abundance of the different progenitor cell subclasses were nearly identical between ISVZ and OSVZ again at P6. Taken together, the analysis of the expression profile for Pax6, Tbr2, and Olig2 indicated the existence of 5 major progenitor cell subclasses in each of the 3 main germinal zones, also that the relative abundance of these populations varies during development, and that they are represented in nearly identical proportions in ISVZ and OSVZ, demonstrating that differences in ontogeny and cytoarchitecture between ISVZ and OSVZ are independent of the expression profile for these transcription factors.

Different Abundance of IRGCs between ISVZ and OSVZ

Next, we examined whether ISVZ and OSVZ may differ in the morphology of their progenitor cells. Previous studies highlighted the relevance of IRGCs in the evolutionary expansion and folding of the mammalian cerebral cortex (Fietz et al. 2010; Hansen et al. 2010; Fietz and Huttner 2011; Lui et al. 2011; Reillo et al. 2011; Shitamukai et al. 2011; Wang et al. 2011). This newly identified type of cortical progenitor resembles classical radial glia except for the apical process contacting the ventricular surface of the telencephalon, which is missing in IRGCs (Fietz et al. 2010; Hansen et al. 2010; Reillo et al. 2011; Shitamukai et al. 2011; Wang et al. 2011). Although IRGCs have been demonstrated to exist in OSVZ (Fietz et al. 2010; Hansen et al. 2010; Reillo et al. 2011) and ISVZ (Reillo et al. 2011), their ontogenetic origin and relative abundance have not been compared across layers, so we tested whether ISVZ and OSVZ might differ at the level of IRGCs. IRGCs and their unique morphology are revealed by anti-phosphovimentin (PhVim) antibodies, which label the cytoplasm of mitotic radial glia–like cells (Weissman et al. 2003; Martinez-Cerdeno et al. 2006; Fietz et al. 2010; Hansen et al. 2010; Wang et al. 2011). We found numerous PhVim+ cells with a basal process in the VZ from E30 to P6 (Fig. 9*A–F*), consistent with the radial glia nature of VZ progenitors in ferret (Weissman et al. 2003; Reillo et al. 2011). In contrast, in the SVZ, we could not detect PhVim+ cells with a basal process (IRGCs) until E38 (Fig. 9*G,H*). These first IRGCs were observed simultaneously in both ISVZ and OSVZ (Fig. 9*G,H*), despite of the delayed emergence of the OSVZ compared with the ISVZ (Figs 1–3).

Quantitative analysis of PhVim+ cells showed that their relative abundance increased significantly in both ISVZ and OSVZ between E38 and P6 but also that the increase in OSVZ was almost twice as in ISVZ (OSVZ, E38, 13.1 ± 2.6%, P6, 38.4 ± 2.1%; ISVZ, E38, 20.7 ± 0.3%, P6, 33.4 ± 4.7%; Supplementary Fig. 4), which resulted on proliferation in OSVZ quickly becoming preponderant over the other zones. A similar situation was observed when considering only PhVim+ cells with a basal process (IRGCs), as between E38 and P6, these also increased rapidly in both germinal zones but much more dramatically in OSVZ than in ISVZ (OSVZ, from 10.4 ± 1.1% to 38.4 ± 2.1%, 3.5-fold increase; ISVZ, from 13.2 ± 0.4% to 27.9 ± 4.2%, 2.1-fold increase; Fig. 9*K*). In contrast, the relative abundance of PhVim+ cells without a basal process between E38 and P6 remained constant in ISVZ (0.96-fold change), while it increased in the OSVZ (1.9-fold; Supplementary Fig. 4), although this increase was much less than for IRGCs (see above). Comparison of the relative abundance of PhVim+ cells with or without a basal process also showed differences between ISVZ and OSVZ, where the proportion of IRGCs was significantly larger in the OSVZ than in ISVZ at E38 and P6 (Fig. 9*L*).

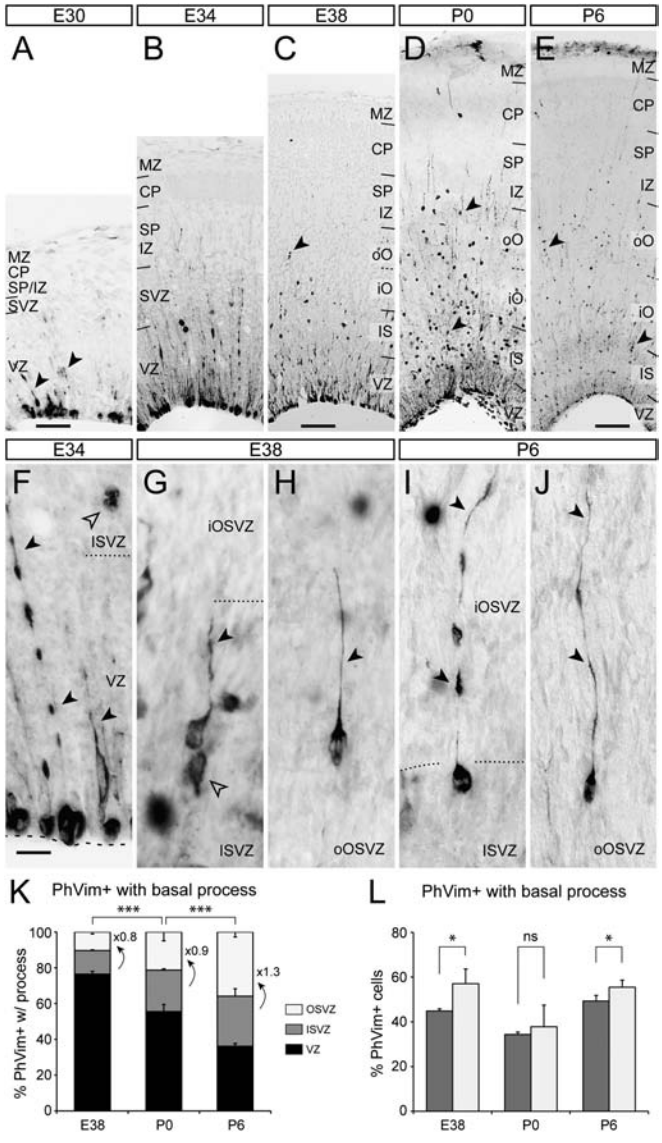

Figure 9. Ontogeny of fosfovimentin expression in the presumptive visual cortex. (*A–E*) Details across the cortical depth of representative stains for fosfovimentin at embryonic and early postnatal stages. Arrowheads indicate examples of cells with a basal process. iO, inner OSVZ; oO, outer OSVZ; and IZ, ISVZ. (*F–J*) High magnification of cells with a basal process (solid arrowheads) in the VZ (*F*), ISVZ (*G* and *I*), and OSVZ (*H* and *J*) at the ages indicated. Open arrowheads in (*F* and *G*) point at examples of cells without a basal process in ISVZ. (*K*) Quantification of the laminar distribution of fosfovimentin (PhVim) positive cells with a basal process between E38 and P6. Numbers within graph indicate fold difference of OSVZ with respect to ISVZ. E38, $n = 775$ cells, 2 animals; P0, $n = 501$ cells, 3 animals; and P6, $n = 1481$ cells, 3 animals. (*L*) Proportion of PhVim+ cells in ISVZ and OSVZ that have a basal process. Legend as in (*K*). At E38 and P6, cells with a basal process were more abundant in OSVZ than in ISVZ. $n = 3$ animals per age, 3 sections per animal (E38, $n = 297$ cells in ISVZ, 186 cells in OSVZ; P0, $n = 342$ cells in ISVZ, 288 cells in OSVZ; and P6, $n = 839$ cells in ISVZ, 958 cells in OSVZ. *** $P < 0.001$; * $P < 0.05$; ns, not significant; chi-square test. Scale bar—50 μm (*A* and *B*), 150 μm (*C* and *D*), 200 μm (*E*), and 15 μm (*F–J*).

Taken together, our observations strongly suggested that IRGCs may only appear in the ferret occipital cortex as late as E38, and our quantitative analyses are consistent with previous studies indicating that IRGC abundance increases during the first postnatal week in the prospective visual cortex of the ferret (Reillo et al. 2011). In addition, we found that ISVZ and OSVZ differ in both abundance and dynamics of their IRGC progenitor population.

Cell Cycle Kinetics of Progenitors Differ Between Cortical Germinal Layers

To further investigate additional differences between ISVZ and OSVZ, we next analyzed the proliferation dynamics and mitotic properties of progenitors in these layers, as such features have been shown to vary between VZ and SVZ and during cortical development (Takahashi et al. 1995a, 1995b; Haydar et al. 2003; Noctor et al. 2008; Fietz et al. 2010). Orientation of the cleavage plane during mitosis of neocortical progenitors determines the symmetric or asymmetric inheritance of particular cellular components, including apical complex proteins and the apical or basal process of neuroepithelial cells (Kosodo et al. 2004; Gotz and Huttner 2005; Huttner and Kosodo 2005; Fish et al. 2008; Fietz et al. 2010; Hansen et al. 2010; Reillo et al. 2011; Shitamukai et al. 2011; Wang et al. 2011), and has also been associated with different types of progenitor cells (Noctor et al. 2008). To gain further insight into differences between progenitors in the different germinal layers of the developing ferret cerebral cortex, we measured their cleavage plane orientation during mitosis, as evidenced by PH3 staining. Because dividing cells frequently rotate their mitotic plate during metaphase, but not in anaphase (Haydar et al. 2003), we only considered PH3+ cells in anaphase and early telophase (Fig. 10*A*–*C*) (Fietz et al. 2010). We found at P0 the majority of ventricular mitoses to occur preferentially in the vertical plane, nearly perpendicular to the ventricular surface (Fig. 10*D*). At later stages, in contrast, the orientation of mitoses shifted dramatically, occurring randomly at P2, and nearly parallel to the ventricular surface at P6 (Fig. 10*D*).

Mitotic cleavage plane orientation is usually measured with respect to the ventricular surface of the telencephalon (VZ surface) because molecular cell fate determinants have been presumed to distribute with respect to this plane (Chenn and McConnell 1995; Gotz and Huttner 2005), although there are studies contradicting this notion (Knoblich 2008; Konno et al. 2008; Neumuller and Knoblich 2009; Shitamukai et al. 2011). In any case, this does not apply to progenitor cells that are not anchored to the apical surface of the telencephalon, such as multipolar IPCs and IRGCs (Noctor et al. 2004, 2008; Fietz et al. 2010; Hansen et al. 2010; Reillo et al. 2011). Thus, we reasoned that non-VZ progenitors may have no information on the position of the ventricular surface, and hence, they may distribute their potential cell fate determinants independently of it. In this scenario, radial glia fibers may provide the only spatial reference for non-VZ progenitors, and these might orient their mitoses with respect to the direction of this radial axis. As proof of principle, we measured the orientation of VZ mitoses with respect to the radial fiber scaffold, revealed by anti-vimentin stain (Fig. 10*A*′). As expected, we found VZ mitoses to be largely parallel to radial fibers at P0 and largely perpendicular to them at P6 (Fig. 10*D*). Using this same criterion, we found that ISVZ and OSVZ mitoses had near-random distributions at all ages examined (Fig. 10*D*). Nevertheless, OSVZ mitoses did show a tendency to follow a trend similar to VZ mitoses, with a bias to be parallel to the radial fiber scaffold at P0, randomly oriented at P2, and then biased to a perpendicular orientation at P6 (Fig. 10*D*).

To further define the dynamics of progenitor proliferation, we next focused on measuring the length of the cell cycle and the rate of cell cycle reentry (Takahashi et al. 1995a, 1995b; Lukaszewicz et al. 2005). Cumulative BrdU-labeling experiments allowed us to determine that ISVZ and OSVZ differed in the cell cycle length of their progenitor cells, as the total cell cycle was 15–25% longer in OSVZ and VZ progenitors compared with ISVZ progenitors (Fig. 11*A* and Table 2). We also found that the length of the cell cycle shortened during development in all layers, being 27–36% longer at P0 than at P6 (Fig. 11*A* and Table 2). These results are in agreement with measurements in macaque cerebral cortex along cortical development (Kornack and Rakic 1998) and highlight an important difference from mouse cortical development, where cell cycle length has been shown to gradually increase during development (Takahashi et al. 1995). Changes in cell cycle length of cortical progenitors have been usually attributed to variations in the duration of the G1 phase, both in mouse and macaque monkey (Takahashi et al. 1995; Lukaszewicz et al. 2005; Dehay and Kennedy 2007). In contrast, we found that differences in cell cycle length were mostly due to changes in S-phase, which was 50–52% longer in VZ and 19–24% longer in OSVZ compared with ISVZ (Fig. 11*A* and Table 2). Interestingly, this was in agreement with recent analyses demonstrating that variations in the length of S-phase, but not G1, distinguish among different types of cortical progenitors (Arai et al. 2011).

Finally, another parameter of the cell cycle that characterizes progenitor dynamics is the rate of cell cycle reentry, defined as the frequency of newborn cells continuing as cycling progenitors, as opposed to becoming postmitotic cells (i.e., neurons). We found that both at P0 and P6, the cell cycle reentry was similar in VZ and ISVZ progenitors but 16–38% higher than in OSVZ progenitors (Fig. 11*B*). This indicated that progenitors in OSVZ have a significant tendency to leave the cell cycle more frequently than in the other germinal layers.

Altogether, our findings indicated that OSVZ and ISVZ progenitors differ in a variety of parameters, including total length of their cell cycle, length of S-phase, and also in their rate of cell cycle reentry. In addition, we found that VZ and OSVZ progenitors gradually shifted their mitotic cleavage plane orientation with respect to the radial fiber scaffold between P0 and P6, from parallel to perpendicular, whereas ISVZ progenitors exhibited random mitotic orientations at all ages.

Discussion

Cellular mechanisms underlying the developmental expansion and folding of the cerebral cortex in gyrencephalic mammals have only begun to be identified and are still poorly understood (Lui et al. 2011). Comparative studies across gyrencephalic and lissencephalic species strongly suggest the involvement of distinct germinal layers and types of progenitor cells in this process (Smart et al. 2002; Martinez-Cerdeno et al. 2006; Fietz et al. 2010; Hansen et al. 2010; Reillo et al. 2011). However, the defining features of such germinal layers and cell types, and which of those features are necessary and sufficient for the development of gyrencephaly, regardless of phylogeny, remain unclear. In the present study, we have used the ferret as model

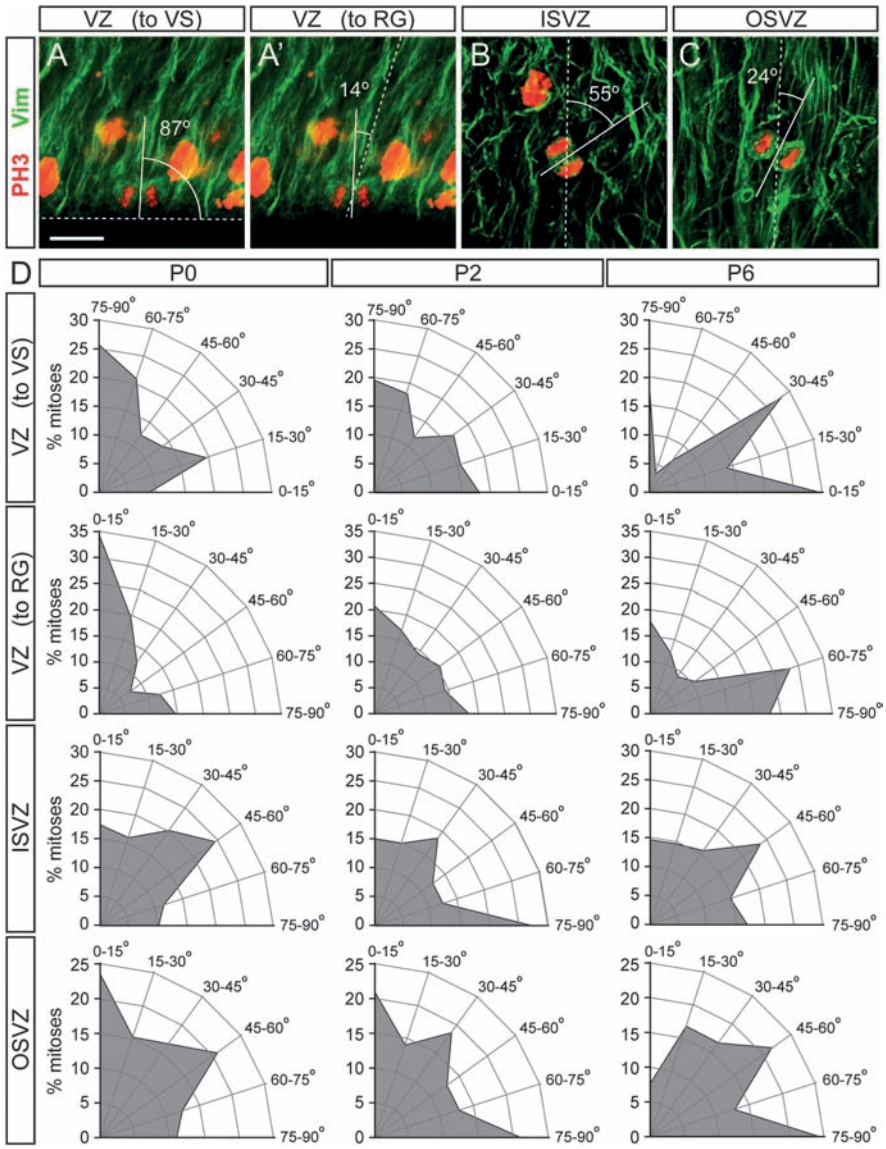

Figure 10. Mitotic cleavage plane orientation varies between germinal layers and during development. (*A–C*) Double stains for PH3 (red) and Vimentin (green) of VZ (*A* and *A'*), ISVZ (*B*), and OSVZ (C) at P0, illustrating the relationship between mitotic plane of telophasic cells (solid line), ventricular surface (VS) (dashed line in *A*), and orientation of radial glia processes (dashed lines in A', B, and C). (*D*) Quantifications of the angle of mitotic division of VZ, ISVZ, and OSVZ progenitors at P0, P2, and P6. Each plot represents the percentage of mitoses found within each range of angles (P0, $n = 82$ mitoses in VZ, 69 in ISVZ, and 75 in OSVZ; P2, $n = 77$ mitoses in VZ, 81 in ISVZ, and 86 in OSVZ; and P6, $n = 57$ mitoses in VZ, 89 in ISVZ, and 78 in OSVZ; 3 animals per group). The angle of each VZ mitosis was measured with respect to the VS and to the direction of radial glia fibers (RG), as indicated. The distributions of mitotic plane values for VZ progenitors varied little between the 2 methods of measurement, although the distribution with respect to RG was most coherent. The orientation of mitotic divisions switched gradually between P0 and P6, from mostly parallel to the radial glia to mostly perpendicular. Scale bar—15 μm (*A–C*).

to demonstrate the existence of 3 distinct germinal layers in the developing cerebral cortex of nonprimate gyrencephalic species: VZ, ISVZ, and OSVZ. We show that these 3 layers share many features with their primate counterparts, including the combinatorial coexpression of several transcription factors such as Pax6, Tbr2, Olig2, and Sox2 in distinct progenitor populations; the abundant presence of IRGCs; and the existence of a cell-sparse subdivision of the OSVZ (iOSVZ) resembling the IFL of primates. But most importantly, our results show that OSVZ and ISVZ are quite different in cytoarchitectonics and certain features of their progenitor cells, demonstrating the limitations of transcription factor expression analysis when it comes to understanding the roles of the different germinal layers in cortical development.

A Multilayered SVZ in a Gyrencephalic Nonprimate

A seminal study on the emergence and distinction of germinal layers in the developing primate cerebral cortex identified the existence of 4 laminar subdivisions in the macaque monkey: VZ, ISVZ, IFL, and OSVZ, overlaid by the OFL, a second fiber-rich layer (Smart et al. 2002). A recent study on the developing cerebral cortex of gyrencephalic nonprimates identified 3 germinative subdivisions based on cell density: VZ, ISVZ, and a vestigial form of the primate OSVZ (Reillo et al. 2011). Here, we have focused on the ferret prospective visual cortex aiming to define the properties and dynamics of these various germinal layers during development and the distinctions between them. Our analyses demonstrate that a very simple ISVZ exists from

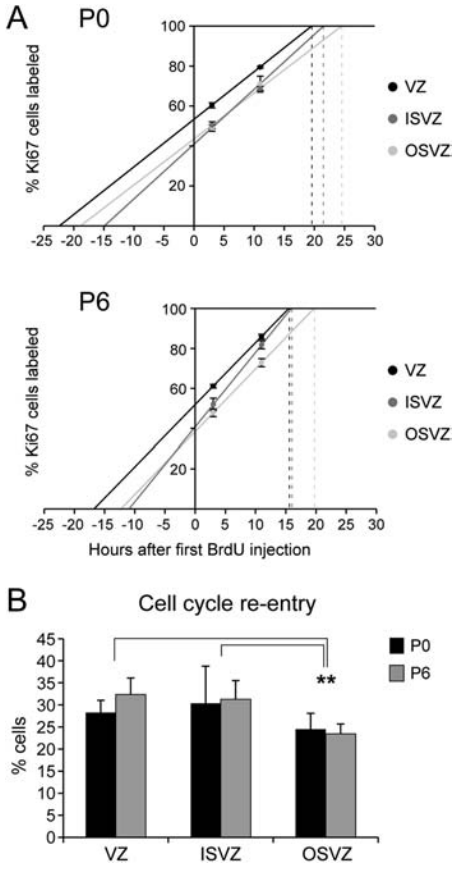

Figure 11. Analysis of cell cycle dynamics of cortical progenitors in the prospective primary visual cortex of ferret. (*A*) Quantifications of cumulative BrdU-labeling experiments in VZ, ISVZ, and OSVZ at P0 and P6 (gray scale dots, as in legend) expressed as percentage of Ki67+ cells positive for BrdU at 3 or 11 h after the first BrdU injection. Statistical significance between layers was tested by a generalized linear model using a binary logistic regression in which the covariates were time and layer. Statistical differences were tested by chi-square test ($P < 0.0001$ for all comparisons between layers for same age and between ages for same layer). The regression line for each data set allowed determination of Tc-s (time at which 100% of Ki67+ cells would be labeled by BrdU; $y = 100$, dashed lines) and Ts (time at which 0% of Ki67+ cells would contain BrdU; $y = 0$). Tc-s + Ts determines the total length of the cell cycle (Tc). (*B*) Quantification of the percentage of VZ, ISVZ, and OSVZ progenitor cells reentering the cell cycle at P0 and P6. Cell cycle reentry was identical between P0 and P6 in all layers, but in OSVZ, it was lower than in ISVZ and VZ. $^{**}P < 0.01$; chi-square test.

Table 2
Measurements of cell cycle length in each of the main germinal layers of the ferret cerebral cortex during the first postnatal week

	P0	P6
VZ		
Tc	**41.96**	**32.25**
Ts	22.31	16.70
Tc-s	19.65	15.56
ISVZ		
Tc	**36.45**	**26.84**
Ts	14.85	10.96
Tc-s	21.59	15.88
OSVZ		
Tc	**42.71**	**33.61**
Ts	18.44	13.08
Tc-s	24.27	20.54

Note: Values indicate hours. Tc, total length of cell cycle; Tc-s, total length of cell cycle without S-phase; and Ts, length of S-phase.

the onset of visual cortex neurogenesis (E30) and that the OSVZ is not distinguishable until 1 week later (E38). This dynamics is similar to that demonstrated in the macaque (Smart et al. 2002), further highlighting the similarities between gyrencephalic primates and nonprimates (Fietz et al. 2010; Fietz and Huttner 2011; Reillo et al. 2011). In spite of the difference in time of emergence between ISVZ and OSVZ, we show that, once generated, these 2 layers have remarkably similar compositions in progenitor cell classes as identified by morphology and coexpression of multiple transcription factors, which suggests that the OSVZ may initially form as a specialized expansion of the ISVZ.

Previous analyses of progenitor cell classes in the developing human cerebral cortex have demonstrated that OSVZ and VZ-ISVZ have a similar composition (Bayatti, Moss, et al. 2008; Mo and Zecevic 2008; Hansen et al. 2010). This led to propose that the OSVZ may be a duplicate of the VZ and ISVZ together, as a strategy to increase neurogenesis and the eventual expansion of the human cerebral cortex (Hansen et al. 2010). Some of our current observations in the ferret also suggested a functional duplicity between ISVZ and OSVZ not only because progenitor cells in these 2 layers have a nearly identical gene expression profile (Fig. 8) but also because the generation of the first IRGCs was simultaneous in both layers (Fig. 9). However, a detailed analysis of other features, such as abundance and dynamics of IRGCs, progenitor cell cycle length, rate of cell cycle reentry, and orientation of mitotic plate, revealed unequivocal differences between these 2 layers and highlighted their uniqueness. This demonstrates that the biology of these complex mixtures of progenitor populations cannot be simplified by the combinatorial analysis of coexpression of a few transcription factors and also that OSVZ is not a mere duplicate of the ISVZ, highlighting that each of these subventricular germinal layers is likely to have distinct and specific roles in cortical development.

Equivalence of Germinal Layers between Gyrencephalic Primates and Nonprimates

To what extent nonprimate species have an equivalent to the highly specialized germinal layers of human and nonhuman primates? In the present study, we provide extensive and compelling evidence on the existence of 3 distinct germinal layers in the developing ferret cerebral cortex. Based on cytoarchitectonics, transcription factor expression, and progenitor cell morphology, we have found that these 3 germinal layers are highly reminiscent of the primate VZ, ISVZ, and OSVZ (Smart et al. 2002; Reillo et al. 2011). However, the developing macaque and human cerebral cortex are also characterized by some other features: IFL, a massive enlargement of the OSVZ, and sustained growth of the SP zone (Sidman and Rakic 1973; Smart and McSherry 1986; Smart et al. 2002; Bayer and Altman 2005). The IFL is a cell-poor zone filled with axon fascicles, which is commonly used to delimit ISVZ from OSVZ at late developmental stages (Smart et al. 2002; Dehay and Kennedy 2007). Although no such distinct layer can be observed in the developing ferret cortex, our analyses demonstrate that the existence of an inner subdivision of the OSVZ (iOSVZ) sharing similarities with the IFL. As opposed to the oOSVZ, progenitor cells in the iOSVZ align in narrow streams flanked by cell-poor spaces, which may be filled by thick bundles of axonal fibers. This situation is highly

reminiscent of the IFL in macaque and human (Smart et al. 2002; Lukaszewicz et al. 2005, 2006), which suggests that the ferret iOSVZ may be a vestigial form of the primate IFL.

Although the IFL is a useful landmark to define the boundary between ISVZ and OSVZ at late stages of primate cortical development, at early stages, well before the appearance of the IFL, cytoarchitectonic criteria are sufficient to distinguish between OSVZ and ISVZ (Smart et al. 2002; Lukaszewicz et al. 2005, 2006; Reillo et al. 2011). Thus, the absence of a distinct IFL in ferret does not preclude the distinction between OSVZ and ISVZ. On the contrary, by applying the same cytoarchitectonic criteria, in combination with transcription factor analysis and cell cycle marker analysis, we provide compelling evidence to distinguish between OSVZ and ISVZ in the developing ferret.

Finally, the massive enlargement of the SP zone observed in primates during corticogenesis (Kostovic and Rakic 1990; Smart et al. 2002) is not paralleled in ferret. While this quantitative difference by itself may already have a profound impact on subsequent events of cortical development, qualitative assessments of the OSVZ and SP zone in the developing macaque and human cerebral cortex demonstrate the existence of an extremely complex mixture of cell types and cellular processes (Smart et al. 2002; Zecevic et al. 2005, 2011; Howard et al. 2006; Bayatti, Moss, et al. 2008; Mo and Zecevic 2009; Hansen et al. 2010; Jakovcevski et al. 2011; Yu and Zecevic 2011) as well as a complex repertoire of progenitor cell behaviors and dynamics (Hansen et al. 2010), which are also likely to play fundamental roles in corticogenesis, and so far, these have not been demonstrated in nonprimates.

Relevance of Germinal Layers and Progenitor Types in Cortical Gyration

Previous studies showed that the enlargement and specialization of the SVZ into very prominent ISVZ and OSVZ distinguishes cortical development in macaque monkey from mouse (Smart et al. 2002; Dehay and Kennedy 2007). We have previously proposed that this may be a phenomenon distinctive and common to all gyrencephalic eutherians and causally related to the development of gyrencephaly (Reillo et al. 2011). This hypothesis is supported by our present findings in ferret, together with our previous observations in other gyrencephalic carnivores, ungulates, and primates, which are in contraposition to lissencephalic rodents, where only the VZ and a relatively thin SVZ are distinguished (Dehay and Kennedy 2007; Reillo et al. 2011). This notion is also supported by findings in metatherians, where 2 or even only one germinal layer have been described so far in their developing cerebral cortex (Cheung et al. 2010; Puzzolo and Mallamaci 2010).

A second distinctive feature between gyrencephalic and lissencephalic brains is the size in surface area of the neuroepithelium at the onset of neurogenesis, which is dramatically larger in ferret, macaque monkey, or human compared with mouse or rat (Sidman and Rakic 1973; Bayer and Altman 1991; Smart et al. 2002; Reillo et al. 2011). These differences support the radial unit hypothesis (Rakic 1995), according to which the evolutionary expansion in cortical surface area resulted from an increase in the number of founder neuroepithelial cells prior to neurogenesis, forming the cortical anlage or VZ. This hypothesis was tested experimentally in a set of genetic manipulations in mouse, where neuroepithelial cells were forced to reenter the cell cycle, resulting in a massive expansion of the VZ progenitor population and a "gyrencephalic" appearance of the transgenic mice (Chenn and Walsh 2002). This study was the first example of how expansion of progenitor populations could be the cellular basis for cortical expansion and gyration (Chenn and Walsh 2002; Siegenthaler et al. 2009). However, this phenotype is different from natural gyrencephaly, where dramatic expansion and folding of the neocortex occur without a proportional expansion and folding of the ventricular surface (Fig. 1). Thus, whereas the importance of the founder progenitor population (VZ) in neocortical expansion is unquestionable, natural gyrencephaly may require the combination of increased VZ proliferation with other developmental processes. Existing evidence (see above) highlights the secondary germinal layers ISVZ and OSVZ as potentially key elements in such cocktail (Kriegstein et al. 2006; Fietz and Huttner 2011; Lui et al. 2011; Reillo et al. 2011).

In this context, the discovery in human and ferret of IRGCs/oRGs, a new class of ISVZ/OSVZ progenitor not previously observed in the SVZ of rodents (Fietz et al. 2010; Hansen et al. 2010; Reillo et al. 2011), seemed to reinforce the relevance of SVZ specializations on cortical expansion and gyration (Fietz and Huttner 2011). However, more recent studies have shown the existence of small numbers of oRG-like progenitor cells in the SVZ of the lissencephalic mouse (Shitamukai et al. 2011; Wang et al. 2011). Although the abundance of oRG-like cells in the developing mouse cortex is so sparse that these do not even constitute a distinct germinal layer, as opposed to ferret or human (Shitamukai et al. 2011; Wang et al. 2011), these findings demonstrate that IRGC/oRGs are not unique to gyrencephalic mammals, and thus, the mere existence of this particular subtype of progenitor is not the key to cortical gyration. Taken together, findings in rodents, carnivores, and primates are consistent with the idea that IRGC/oRG-like cells might have existed in a common mammalian ancestor and that their expansion and the overproliferation of the OSVZ could have been selectively utilized during evolution as means to generate larger and gyrated brains.

Whereas all these observations support a link between prominent ISVZ–OSVZ with high abundance of IRGCs/oRGs and gyrencephaly, larger numbers and diversity of mammalian species need to be analyzed in great detail before general conclusions can be reached. Among these, the analysis of lissencephalic primates, such as the marmoset monkey, and of gyrencephalic rodents and marsupials like the capybara or the wombat, hold promise of a better understanding of cortical folding mechanisms and their evolution.

Origin and Diversity of Cortical Progenitor Cells

Although we are far from understanding the developmental mechanisms that lead to the expansion and folding of the cerebral cortex in larger mammals, significant advances have been made recently demonstrating that these processes are even more complex than previously suspected and involve the interplay between a variety of cell types, genetic programs, and progenitor cell lineages of exquisite complexity (Fietz et al. 2010; Hansen et al. 2010; Fietz and Huttner 2011; Reillo et al. 2011). One issue left unresolved from the original descriptions of IRGCs in ferret and human was their ontogenetic origin (Fietz et al. 2010; Hansen et al. 2010; Reillo et al. 2011). In both ferret and human, IRGCs seemed to have a dual origin depending on the layer: those in the ISVZ appeared generated

from VZ progenitors (Reillo et al. 2011), much like oRGs in rodents (Shitamukai et al. 2011; Wang et al. 2011), whereas those in the OSVZ seemed to be generated only locally by self-amplification (Hansen et al. 2010; Reillo et al. 2011). Here, by monitoring the earliest appearance of IRGCs in the ferret, we show that: 1) they are first generated earlier than previously suspected (Fietz et al. 2010), 2) they are generated simultaneously in both ISVZ and OSVZ, and 3) they are highly abundant from the onset (Fig. 9). Although this may seem to contradict our observations that ISVZ develops earlier than OSVZ in both ferret and human (Bayatti, Moss, et al. 2008, this study, and our I Reillo, V Borrell, unpublished observations), further investigations are clearly needed and should be oriented at providing definite answers to these fundamental questions.

The most systematic characterizations of cortical progenitor subclasses have been done by cell morphology and through the analysis of expression of multiple transcription factors (Englund et al. 2005; Kowalczyk et al. 2009; Arai et al. 2011), in a similar fashion as it was done first in the spinal cord (Pfaff and Kintner 1998; Briscoe et al. 2000; Shirasaki and Pfaff 2002) and later in the basal forebrain (Flames et al. 2007). In the mouse cerebral cortex, this has allowed discriminating between 2 main sets of cortical progenitors: Pax6+/Tbr2–, which include VZ and oVZ radial glia; and Pax6–/Tbr2+, corresponding to SVZ IPCs (Wang et al. 2011). In gyrencephalic mammals, cortical progenitors express Pax6, Tbr2, Sox2, Olig2, and Ascl1 in a nonmutually exclusive manner ([Mo and Zecevic 2008, 2009; Fietz et al. 2010; Hansen et al. 2010; Reillo et al. 2011] and this study), and therefore, the molecular diversity of progenitor cells increases exponentially. Furthermore, our current observations demonstrate that regardless of the combinatorial expression of various transcription factors, cortical progenitors also differ in their dynamics of cell division, including duration of cell cycle, rate of cell cycle reentry, and orientation of mitotic divisions. So, is there a limited diversity to cortical progenitors? We anticipate that a better understanding of the biological relevance of these distinct transcription factors in cortical progenitors, and their mutual transcriptional regulation (Sessa et al. 2008; Sansom et al. 2009), will likely shed light on the numbers and roles of cortical progenitor subtypes. In summary, the evolution of cortical folding specifically, and of cortical complexity at large, appears to have come about in parallel with the specialized and diversified evolution of cortical progenitor cells (Rakic 1995; Lui et al. 2011). Understanding how the different types of progenitor cells interact and how they interplay with migrating neurons and afferent axonal projections holds promise to our understanding of the emergence of the astounding complexity of the mammalian cerebral cortex.

Supplementary Material

Supplementary material can be found at: http://www.cercor.oxfordjournals.org/

Funding

The International Human Frontier Science Program Organization, MICINN (grant BFU2006-08961/BFI, SAF2009-07367) and CONSOLIDER (grant CSD2007-00023) to V.B.

Notes

We thank C. Vegar for outstanding technical assistance and members of our laboratory for helpful discussions. I.R. was recipient of an Formación de Personal Universitario predoctoral fellowship from the Spanish Ministry of Science and Innovation (MICINN). *Conflict of Interest* : None declared.

References

Angevine JB, Sidman RL. 1961. Autoradiographic study of cell migration during histogenesis of cerebral cortex in the mouse. Nature. 192:766–768.

Arai Y, Pulvers JN, Haffner C, Schilling B, Nusslein I, Calegari F, Huttner WB. 2011. Neural stem and progenitor cells shorten S-phase on commitment to neuron production. Nat Commun. 2:154.

Bayatti N, Moss JA, Sun L, Ambrose P, Ward JF, Lindsay S, Clowry GJ. 2008. A molecular neuroanatomical study of the developing human neocortex from 8 to 17 postconceptional weeks revealing the early differentiation of the subplate and subventricular zone. Cereb Cortex. 18:1536–1548.

Bayatti N, Sarma S, Shaw C, Eyre JA, Vouyiouklis DA, Lindsay S, Clowry GJ. 2008. Progressive loss of PAX6, TBR2, NEUROD and TBR1 mRNA gradients correlates with translocation of EMX2 to the cortical plate during human cortical development. Eur J Neurosci. 28:1449–1456.

Bayer SA, Altman J. 1991. Neocortical development. New York: Raven Press.

Bayer SA, Altman J. 2005. The human brain during the second trimester. New York: CRC Press.

Bilguvar K, Ozturk AK, Louvi A, Kwan KY, Choi M, Tatli B, Yalnizoglu D, Tuysuz B, Caglayan AO, Gokben S, et al. 2010. Whole-exome sequencing identifies recessive WDR62 mutations in severe brain malformations. Nature. 467:207–210.

Borrell V, Ruiz M, Del Rio JA, Soriano E. 1999. Development of commissural connections in the hippocampus of reeler mice: evidence of an inhibitory influence of Cajal-Retzius cells. Exp Neurol. 156:268–282.

Boulder Committee 1970. Embryonic vertebrate central nervous system: revised terminology. Anat Rec. 166:257–261.

Briscoe J, Pierani A, Jessell TM, Ericson J. 2000. A homeodomain protein code specifies progenitor cell identity and neuronal fate in the ventral neural tube. Cell. 101:435–445.

Bystron I, Blakemore C, Rakic P. 2008. Development of the human cerebral cortex: Boulder Committee revisited. Nat Rev Neurosci. 9:110–122.

Bystron I, Rakic P, Molnar Z, Blakemore C. 2006. The first neurons of the human cerebral cortex. Nat Neurosci. 9:880–886.

Chenn A, McConnell SK. 1995. Cleavage orientation and the asymmetric inheritance of Notch1 immunoreactivity in mammalian neurogenesis. Cell. 82:631–641.

Chenn A, Walsh CA. 2002. Regulation of cerebral cortical size by control of cell cycle exit in neural precursors. Science. 297:365–369.

Cheung AF, Kondo S, Abdel-Mannan O, Chodroff RA, Sirey TM, Bluy LE, Webber N, DeProto J, Karlen SJ, Krubitzer L, et al. 2010. The subventricular zone is the developmental milestone of a 6-layered neocortex: comparisons in metatherian and eutherian mammals. Cereb Cortex. 20:1071–1081.

deAzevedo LC, Fallet C, Moura-Neto V, Daumas-Duport C, Hedin-Pereira C, Lent R. 2003. Cortical radial glial cells in human fetuses: depth-correlated transformation into astrocytes. J Neurobiol. 55:288–298.

Dehay C, Kennedy H. 2007. Cell-cycle control and cortical development. Nat Rev Neurosci. 8:438–450.

Dorus S, Vallender EJ, Evans PD, Anderson JR, Gilbert SL, Mahowald M, Wyckoff GJ, Malcom CM, Lahn BT. 2004. Accelerated evolution of nervous system genes in the origin of Homo sapiens. Cell. 119:1027–1040.

Engel AK, Muller CM. 1989. Postnatal development of vimentin-immunoreactive radial glial cells in the primary visual cortex of the cat. J Neurocytol. 18:437–450.

Englund C, Fink A, Lau C, Pham D, Daza RA, Bulfone A, Kowalczyk T, Hevner RF. 2005. Pax6, Tbr2, and Tbr1 are expressed sequentially by radial glia, intermediate progenitor cells, and postmitotic neurons in developing neocortex. J Neurosci. 25:247–251.

Evans PD, Anderson JR, Vallender EJ, Gilbert SL, Malcom CM, Dorus S, Lahn BT. 2004. Adaptive evolution of ASPM, a major determinant of cerebral cortical size in humans. Hum Mol Genet. 13:489–494.

Fietz SA, Huttner WB. 2011. Cortical progenitor expansion, self-renewal and neurogenesis-a polarized perspective. Curr Opin Neurobiol. 21:23–35.

Fietz SA, Kelava I, Vogt J, Wilsch-Brauninger M, Stenzel D, Fish JL, Corbeil D, Riehn A, Distler W, Nitsch R, et al. 2010. OSVZ progenitors of human and ferret neocortex are epithelial-like and expand by integrin signaling. Nat Neurosci. 13:690–699.

Fish JL, Dehay C, Kennedy H, Huttner WB. 2008. Making bigger brains—the evolution of neural-progenitor-cell division. J Cell Sci. 121:2783–2793.

Flames N, Pla R, Gelman DM, Rubenstein JL, Puelles L, Marin O. 2007. Delineation of multiple subpallial progenitor domains by the combinatorial expression of transcriptional codes. J Neurosci. 27:9682–9695.

Gilbert SL, Dobyns WB, Lahn BT. 2005. Genetic links between brain development and brain evolution. Nat Rev Genet. 6:581–590.

Gotz M, Huttner WB. 2005. The cell biology of neurogenesis. Nat Rev Mol Cell Biol. 6:777–788.

Hansen DV, Lui JH, Parker PR, Kriegstein AR. 2010. Neurogenic radial glia in the outer subventricular zone of human neocortex. Nature. 464:554–561.

Haubensak W, Attardo A, Denk W, Huttner WB. 2004. Neurons arise in the basal neuroepithelium of the early mammalian telencephalon: a major site of neurogenesis. Proc Natl Acad Sci U S A. 101:3196–3201.

Haydar TF, Ang E, Jr, Rakic P. 2003. Mitotic spindle rotation and mode of cell division in the developing telencephalon. Proc Natl Acad Sci U S A. 100:2890–2895.

Hevner RF, Hodge RD, Daza RA, Englund C. 2006. Transcription factors in glutamatergic neurogenesis: conserved programs in neocortex, cerebellum, and adult hippocampus. Neurosci Res. 55:223–233.

Howard B, Chen Y, Zecevic N. 2006. Cortical progenitor cells in the developing human telencephalon. Glia. 53:57–66.

Huttner WB, Kosodo Y. 2005. Symmetric versus asymmetric cell division during neurogenesis in the developing vertebrate central nervous system. Curr Opin Cell Biol. 17:648–657.

Jackson CA, Peduzzi JD, Hickey TL. 1989. Visual cortex development in the ferret. I. Genesis and migration of visual cortical neurons. J Neurosci. 9:1242–1253.

Jakovcevski I, Mayer N, Zecevic N. 2011. Multiple origins of human neocortical interneurons are supported by distinct expression of transcription factors. Cereb Cortex. 21:1771–1782.

Knoblich JA. 2008. Mechanisms of asymmetric stem cell division. Cell. 132:583–597.

Konno D, Shioi G, Shitamukai A, Mori A, Kiyonari H, Miyata T, Matsuzaki F. 2008. Neuroepithelial progenitors undergo LGN-dependent planar divisions to maintain self-renewability during mammalian neurogenesis. Nat Cell Biol. 10:93–101.

Kornack DR, Rakic P. 1998. Changes in cell-cycle kinetics during the development and evolution of primate neocortex. Proc Natl Acad Sci U S A. 95:1242–1246.

Kosodo Y, Roper K, Haubensak W, Marzesco AM, Corbeil D, Huttner WB. 2004. Asymmetric distribution of the apical plasma membrane during neurogenic divisions of mammalian neuroepithelial cells. EMBO J. 23:2314–2324.

Kostovic I, Rakic P. 1990. Developmental history of the transient subplate zone in the visual and somatosensory cortex of the macaque monkey and human brain. J Comp Neurol. 297:441–470.

Kowalczyk T, Pontious A, Englund C, Daza RA, Bedogni F, Hodge R, Attardo A, Bell C, Huttner WB, Hevner RF. 2009. Intermediate neuronal progenitors (basal progenitors) produce pyramidal-projection neurons for all layers of cerebral cortex. Cereb Cortex. 19:2439–2450.

Kriegstein A, Noctor S, Martinez-Cerdeno V. 2006. Patterns of neural stem and progenitor cell division may underlie evolutionary cortical expansion. Nat Rev Neurosci. 7:883–890.

Letinic K, Zoncu R, Rakic P. 2002. Origin of GABAergic neurons in the human neocortex. Nature. 417:645–649.

Levitt P, Rakic P. 1980. Immunoperoxidase localization of glial fibrillary acidic protein in radial glial cells and astrocytes of the developing rhesus monkey brain. J Comp Neurol. 193:815–840.

Lui JH, Hansen DV, Kriegstein AR. 2011. Development and evolution of the human neocortex. Cell. 146:18–36.

Lukaszewicz A, Cortay V, Giroud P, Berland M, Smart I, Kennedy H, Dehay C. 2006. The concerted modulation of proliferation and migration contributes to the specification of the cytoarchitecture and dimensions of cortical areas. Cereb Cortex. 1(Suppl 16):i26–i34.

Lukaszewicz A, Savatier P, Cortay V, Giroud P, Huissoud C, Berland M, Kennedy H, Dehay C. 2005. G1 phase regulation, area-specific cell cycle control, and cytoarchitectonics in the primate cortex. Neuron. 47:353–364.

Malatesta P, Hartfuss E, Gotz M. 2000. Isolation of radial glial cells by fluorescent-activated cell sorting reveals a neuronal lineage. Development. 127:5253–5263.

Martinez-Cerdeno V, Noctor SC, Kriegstein AR. 2006. The role of intermediate progenitor cells in the evolutionary expansion of the cerebral cortex. Cereb Cortex. 1(Suppl 16):i152–i161.

Mekel-Bobrov N, Gilbert SL, Evans PD, Vallender EJ, Anderson JR, Hudson RR, Tishkoff SA, Lahn BT. 2005. Ongoing adaptive evolution of ASPM, a brain size determinant in Homo sapiens. Science. 309:1720–1722.

Mo Z, Moore AR, Filipovic R, Ogawa Y, Kazuhiro I, Antic SD, Zecevic N. 2007. Human cortical neurons originate from radial glia and neuron-restricted progenitors. J Neurosci. 27:4132–4145.

Mo Z, Zecevic N. 2008. Is Pax6 critical for neurogenesis in the human fetal brain? Cereb Cortex. 18:1455–1465.

Mo Z, Zecevic N. 2009. Human fetal radial glia cells generate oligodendrocytes in vitro. Glia. 57:490–498.

Molnar Z, Vasistha NA, Garcia-Moreno F. 2011. Hanging by the tail: progenitor populations proliferate. Nat Neurosci. 14:538–540.

Neal J, Takahashi M, Silva M, Tiao G, Walsh CA, Sheen VL. 2007. Insights into the gyrification of developing ferret brain by magnetic resonance imaging. J Anat. 210:66–77.

Neumuller RA, Knoblich JA. 2009. Dividing cellular asymmetry: asymmetric cell division and its implications for stem cells and cancer. Genes Dev. 23:2675–2699.

Nicholas AK, Khurshid M, Desir J, Carvalho OP, Cox JJ, Thornton G, Kausar R, Ansar M, Ahmad W, Verloes A, et al. 2010. WDR62 is associated with the spindle pole and is mutated in human microcephaly. Nat Genet. 42:1010–1014.

Noctor SC, Flint AC, Weissman TA, Dammerman RS, Kriegstein AR. 2001. Neurons derived from radial glial cells establish radial units in neocortex. Nature. 409:714–720.

Noctor SC, Martinez-Cerdeno V, Ivic L, Kriegstein AR. 2004. Cortical neurons arise in symmetric and asymmetric division zones and migrate through specific phases. Nat Neurosci. 7:136–144.

Noctor SC, Martinez-Cerdeno V, Kriegstein AR. 2008. Distinct behaviors of neural stem and progenitor cells underlie cortical neurogenesis. J Comp Neurol. 508:28–44.

Pfaff S, Kintner C. 1998. Neuronal diversification: development of motor neuron subtypes. Curr Opin Neurobiol. 8:27–36.

Pollard KS, Salama SR, Lambert N, Lambot MA, Coppens S, Pedersen JS, Katzman S, King B, Onodera C, Siepel A, et al. 2006. An RNA gene expressed during cortical development evolved rapidly in humans. Nature. 443:167–172.

Puzzolo E, Mallamaci A. 2010. Cortico-cerebral histogenesis in the opossum Monodelphis domestica: generation of a hexalaminar neocortex in the absence of a basal proliferative compartment. Neural Dev. 5:8.

Rakic P. 1988. Specification of cerebral cortical areas. Science. 241:170–176.

Rakic P. 1995. A small step for the cell, a giant leap for mankind: a hypothesis of neocortical expansion during evolution. Trends Neurosci. 18:383–388.

Rakic P. 2009. Evolution of the neocortex: a perspective from developmental biology. Nat Rev Neurosci. 10:724–735.
Rakic S, Zecevic N. 2003. Emerging complexity of layer I in human cerebral cortex. Cereb Cortex. 13:1072–1083.
Ramón y Cajal S. 1911. Histologie du Système Nerveux de l'Homme et des Vertébrés. Paris: Maloine.
Reillo I, de Juan Romero C, Garcia-Cabezas MA, Borrell V. 2011. A role for intermediate radial glia in the tangential expansion of the mammalian cerebral cortex. Cereb Cortex. 21:1674–1694.
Ross ME, Walsh CA. 2001. Human brain malformations and their lessons for neuronal migration. Annu Rev Neurosci. 24:1041–1070.
Sansom SN, Griffiths DS, Faedo A, Kleinjan DJ, Ruan Y, Smith J, van Heyningen V, Rubenstein JL, Livesey FJ. 2009. The level of the transcription factor Pax6 is essential for controlling the balance between neural stem cell self-renewal and neurogenesis. PLoS Genet. 5:e1000511.
Sauer ME, Walker BE. 1959. Radioautographic study of interkinetic nuclear migration in the neural tube. Proc Soc Exp Biol Med. 101:557–560.
Schmechel DE, Rakic P. 1979. A Golgi study of radial glial cells in developing monkey telencephalon: morphogenesis and transformation into astrocytes. Anat Embryol (Berl). 156:115–152.
Sessa A, Mao CA, Hadjantonakis AK, Klein WH, Broccoli V. 2008. Tbr2 directs conversion of radial glia into basal precursors and guides neuronal amplification by indirect neurogenesis in the developing neocortex. Neuron. 60:56–69.
Sheen VL, Walsh CA. 2003. Developmental genetic malformations of the cerebral cortex. Curr Neurol Neurosci Rep. 3:433–441.
Shirasaki R, Pfaff SL. 2002. Transcriptional codes and the control of neuronal identity. Annu Rev Neurosci. 25:251–281.
Shitamukai A, Konno D, Matsuzaki F. 2011. Oblique radial glial divisions in the developing mouse neocortex induce self-renewing progenitors outside the germinal zone that resemble primate outer subventricular zone progenitors. J Neurosci. 31:3683–3695.
Sidman RL, Rakic P. 1973. Neuronal migration, with special reference to developing human brain: a review. Brain Res. 62:1–35.
Siegenthaler JA, Ashique AM, Zarbalis K, Patterson KP, Hecht JH, Kane MA, Folias AE, Choe Y, May SR, Kume T, et al. 2009. Retinoic acid from the meninges regulates cortical neuron generation. Cell. 139:597–609.
Smart IH, Dehay C, Giroud P, Berland M, Kennedy H. 2002. Unique morphological features of the proliferative zones and postmitotic compartments of the neural epithelium giving rise to striate and extrastriate cortex in the monkey. Cereb Cortex. 12:37–53.
Smart IH, McSherry GM. 1986. Gyrus formation in the cerebral cortex of the ferret. II. Description of the internal histological changes. J Anat. 147:27–43.
Takahashi T, Misson JP, Caviness VS, Jr. 1990. Glial process elongation and branching in the developing murine neocortex: a qualitative and quantitative immunohistochemical analysis. J Comp Neurol. 302:15–28.
Takahashi T, Nowakowski RS, Caviness VS, Jr. 1993. Cell cycle parameters and patterns of nuclear movement in the neocortical proliferative zone of the fetal mouse. J Neurosci. 13:820–833.
Takahashi T, Nowakowski RS, Caviness VS, Jr. 1995a. Early ontogeny of the secondary proliferative population of the embryonic murine cerebral wall. J Neurosci. 15:6058–6068.
Takahashi T, Nowakowski RS, Caviness VS, Jr. 1995b. The cell cycle of the pseudostratified ventricular epithelium of the embryonic murine cerebral wall. J Neurosci. 15:6046–6057.
Tekki-Kessaris N, Woodruff R, Hall AC, Gaffield W, Kimura S, Stiles CD, Rowitch DH, Richardson WD. 2001. Hedgehog-dependent oligodendrocyte lineage specification in the telencephalon. Development. 128:2545–2554.
Voigt T. 1989. Development of glial cells in the cerebral wall of ferrets: direct tracing of their transformation from radial glia into astrocytes. J Comp Neurol. 289:74–88.
Wang X, Tsai JW, Lamonica B, Kriegstein AR. 2011. A new subtype of progenitor cell in the mouse embryonic neocortex. Nat Neurosci. 14:555–561.
Weissman T, Noctor SC, Clinton BK, Honig LS, Kriegstein AR. 2003. Neurogenic radial glial cells in reptile, rodent and human: from mitosis to migration. Cereb Cortex. 13:550–559.
Welker W. 1990. Why does cerebral cortex fissure and fold? A review of determinants of gyri and sulci. In: Peters A, Jones EG, editors. Cerebral cortex. New York: Plenum Press. p. 3–136.
Yu TW, Mochida GH, Tischfield DJ, Sgaier SK, Flores-Sarnat L, Sergi CM, Topcu M, McDonald MT, Barry BJ, Felie JM, et al. 2010. Mutations in WDR62, encoding a centrosome-associated protein, cause microcephaly with simplified gyri and abnormal cortical architecture. Nat Genet. 42:1015–1020.
Yu X, Zecevic N. 2011. Dorsal radial glial cells have the potential to generate cortical interneurons in human but not in mouse brain. J Neurosci. 31:2413–2420.
Zecevic N. 2004. Specific characteristic of radial glia in the human fetal telencephalon. Glia. 48:27–35.
Zecevic N, Chen Y, Filipovic R. 2005. Contributions of cortical subventricular zone to the development of the human cerebral cortex. J Comp Neurol. 491:109–122.
Zecevic N, Hu F, Jakovcevski I. 2011. Interneurons in the developing human neocortex. Dev Neurobiol. 71:18–33.